AD-A121 319 DISCLINATIONS IN CARBON-CARBON COMPOSITES(U) ACUREX 1/1
CORP MOUNTAIN VIEW CA J E ZIMMER ET AL. SEP 82
TR-82-24/ATD N00014-81-C-0641

UNCLASSIFIED F/G 11/4 NL

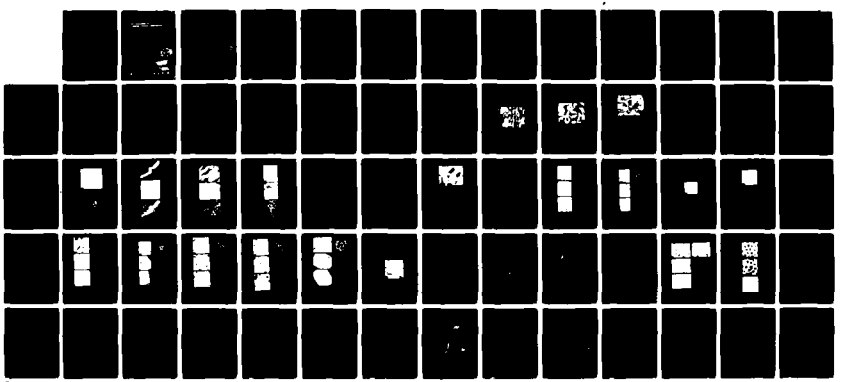

END
DATE FILMED
DTIC

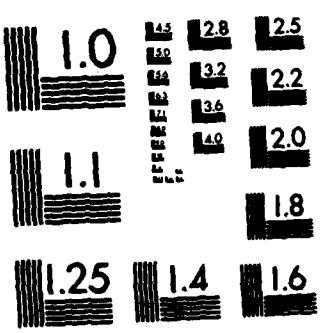

UNCLASSIFIED

SECURITY CLASSIFICATION OF THIS PAGE (When Data Entered)

REPORT DOCUMENTATION PAGE	READ INSTRUCTIONS BEFORE COMPLETING FORM
1. REPORT NUMBER	2. GOVT ACCESSION NO. A121319 / 3. RECIPIENT'S CATALOG NUMBER
4. TITLE (and Subtitle) Disclinations in Carbon-Carbon Composites	5. TYPE OF REPORT & PERIOD COVERED Interim Technical Report July 1981 -- July 1982
	6. PERFORMING ORG. REPORT NUMBER TR-82-24/ATD
7. AUTHOR(s) J. E. Zimmer and R. L. Weitz	8. CONTRACT OR GRANT NUMBER(s) N00014-81-C-0641
9. PERFORMING ORGANIZATION NAME AND ADDRESS Acurex Corporation, Aerotherm Division 485 Clyde Avenue Mountain View, CA 94042	10. PROGRAM ELEMENT, PROJECT, TASK AREA & WORK UNIT NUMBERS
11. CONTROLLING OFFICE NAME AND ADDRESS Office of Naval Research 800 North Quincy Street Arlington, VA 22217	12. REPORT DATE September 1982
	13. NUMBER OF PAGES 82
14. MONITORING AGENCY NAME & ADDRESS(if different from Controlling Office)	15. SECURITY CLASS. (of this report) Unclassified
	15a. DECLASSIFICATION/DOWNGRADING SCHEDULE

16. DISTRIBUTION STATEMENT (of this Report)

Approved for public release

17. DISTRIBUTION STATEMENT (of the abstract entered in Block 20, if different from Report)

18. SUPPLEMENTARY NOTES

19. KEY WORDS (Continue on reverse side if necessary and identify by block number)

Disclinations
Carbonaceous mesophase
Discotic nematic liquid crystal
Carbon-carbon composite
Graphite-fiber bundles
Crack propagation
Fracture toughness

20. ABSTRACT (Continue on reverse side if necessary and identify by block number)

Disclinations are prominent in the matrix microstructure of carbon-carbon composites and are introduced via the formation of the carbonaceous mesophase, a discotic nematic liquid crystal. The structure-sensitive physical properties of these composites are expected to be related to their microstructure and the disclination structures in this microstructure. The objectives of this research are to identify and classify the disclination structures in the matrix of carbon-carbon composites and to determine the relationship of the disclinations to the fracture behavior of the composite matrix.

DD FORM 1 JAN 73 1473 EDITION OF 1 NOV 65 IS OBSOLETE

UNCLASSIFIED

SECURITY CLASSIFICATION OF THIS PAGE (When Data Entered)

For arrays of disclinations in the carbonaceous mesophase, neighboring disclinations are of opposite sign and the total strength of an array tends to zero, as shown with the use of optical micrography. The strength S of a disclination is a measure of the amount of rotational distortion ($2\pi S$) associated with each disclination.

Crack propagation in the carbonaceous mesophase has been studied with the use of optical micrography and a wedge-opening specimen designed to produce incremental crack growth. The disclinations were shown to control the crack path, and to stop and divert the crack path. This evidence indicates that the disclinations in the carbonaceous mesophase contribute to the high work of fracture of graphitic materials by crack blunting, crack diverting and energy absorption.

The disclinations present in the matrix among the graphite filaments in a composite fiber bundle have been identified and classified. The mesophase aligns parallel to the surface of the graphite filaments in a sheath; this alignment and the pattern or arrays of filaments prescribes the type of negative wedge disclination in the matrix. Disclinations of strength $S = -1/2$ exist in triangular arrays of filaments. Disclinations of strength $S = -1$ exist in square arrays. The first evidence of disclinations of strength $S = -2$, as found in hexagonal arrays of filaments, is presented.

FOREWORD

This is the first annual report on a program to study the disclinations in carbon-carbon composites. The work is supported by the Office of Naval Research under contract N00014-81-C-0641. Dr. L. H. Peebles, Jr. is the Scientific Officer; his interest and support are gratefully acknowledged. Also, the assistance of Dr. C. J. Wolf and Mr. V. Kulkarni, Acurex Corporation, and the invigorating consultation with Dr. J. L. White, the Aerospace Corporation, are greatly appreciated.

TABLE OF CONTENTS

LIST OF ILLUSTRATIONS

LIST OF ILLUSTRATIONS (CONTINUED)

LIST OF ILLUSTRATIONS (CONCLUDED)

INTRODUCTION

Disclinations are prominent in the microstructure of carbon-carbon composites, the principal material for thermal protection systems, such as rocket nozzles and reentry vehicle nosetips, and for high-temperature, structural components for turbine engines and tactical missiles. Disclinations are rotational elastic distortions in the graphite matrix of these composites introduced when the matrix was formed via the carbonaceous mesophase, a discotic nematic liquid crystal. The association of disclinations with the microstructure of carbon-carbon composites implies a relationship between the disclinations and the structure-sensitive physical properties of these composites. Thus, basic research is needed to not only understand the topological aspects of disclinations, but also to understand the disclination structures in carbon-carbon composites and the role of these disclinations in controlling the physical properties of these composites.

Carbon-carbon composites have graphitic matrices reinforced with high-strength, high-modulus graphite fibers from rayon, polyacrylonitrile or mesophase pitch. These composites exhibit some unique properties: their elastic modulus at room temperature is retained at elevated temperatures, their volumetric thermal expansion is quite low and they have good fracture toughness. These properties exceed those of other ceramic materials with crystal lattices that do not contain disclinations. Disclinations are inherent in the carbon-carbon composites, since their microstructure is formed

during the transformation by pyrolysis of the matrix precursors such as petroleum and coal-tar pitches to the carbonaceous mesophase. Disclinations can exist in this liquid crystal as the high rotational strains of the disclinations are reduced by flow of the oriented molecules of the liquid crystal.

The objectives of this basic research on the disclinations in carbon-carbon composites are to identify and classify the disclination structures in the matrix of carbon-carbon composites and to determine the relationship of the disclinations to the fracture behavior of the composite matrix.

The specific areas of research which are described in this report are the following: observation of the types and arrangement of disclinations in a disclination array in the carbonaceous mesophase; observation of crack propagation in the carbonaceous mesophase and the relation of the crack path to the disclination structures; and the identification and classification of the disclinations in the matrix in a carbon-fiber bundle in a carbon-carbon composite.

BACKGROUND

The carbonaceous mesophase is a unique liquid crystal formed during the pyrolysis of those organic materials that yield graphitizable cokes or chars [1, 2]. In the temperature range of 400° to 500°C, polymerization reactions occur to build large, disklike, polynuclear aromatic molecules, that, upon reaching molecular weights in the neighborhood of 1,400, condense in parallel arrays and precipitate from the molten pitch as a liquid crystal, the carbonaceous mesophase. Initially, this mesophase forms as small spherules of simple structure, but, after coalescence to viscous bulk mesophase, quite complex morphologies are developed and eventually frozen-in as the pyrolyzing mass hardens to a coke. The carbonaceous mesophase has the structural characteristics of a discotic nematic liquid crystal -- an array of disklike molecules that tend to lie parallel to each other and display long-range orientational order, but are not required to be in point-to-point registry to adjacent molecules [3]. This liquid crystal is shown schematically in Figure 1. Several possible molecular models are shown, based on the analysis of the mesophase by infrared spectroscopy, nuclear magnetic resonance spectroscopy and vapor pressure osmometry [4].

In the liquid-crystal stage of pyrolysis, the basic morphologies of graphitic materials are established through spherule coalescence and deformation of the mesophase. These complex lamelliform morphologies necessarily contain structural discontinuities, that is, disclinations, in the

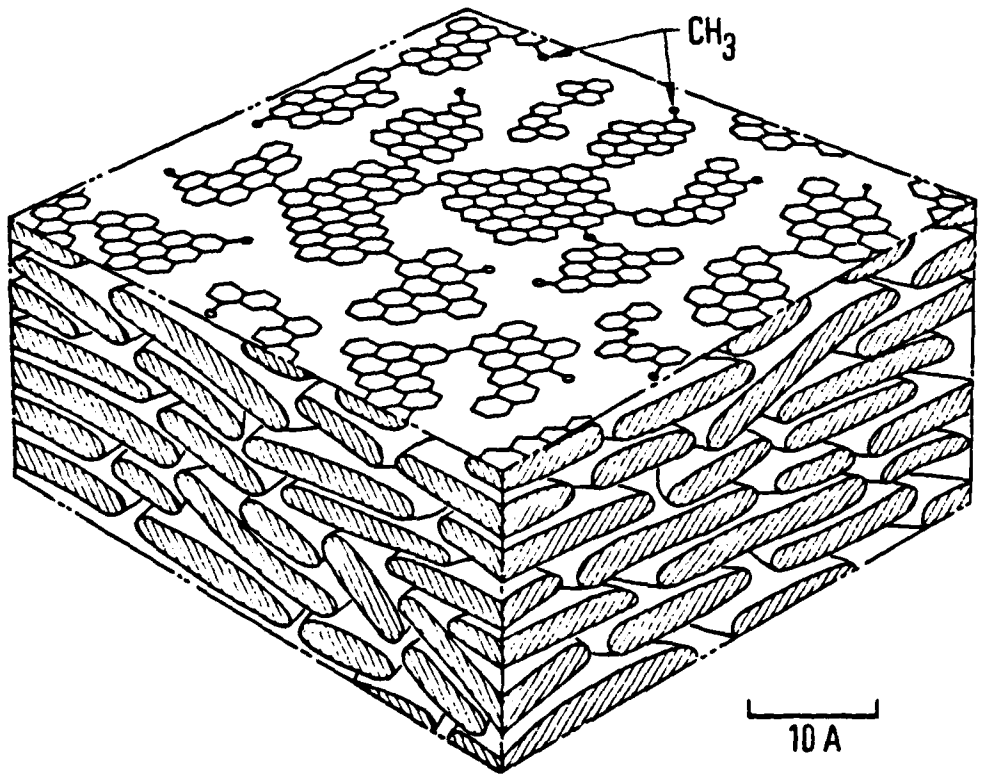

Figure 1. Schematic model of the carbonaceous mesophase, a discotic nematic liquid crystal.

parallel stacking of the aromatic molecules. On a local scale, the parallel stacking in the mesophase is retained throughout a region of material. However, the orientation of the stacking changes continuously as the molecule layers bend, splay and twist, and map out singly and doubly curved surfaces. Topologically, space cannot be filled completely by these curved regions of stacked molecules and thus disclinations exist as the discontinuities in this complex morphology. The disclinations are characterized by a rotation vector of multiples of π, as described by the two-fold symmetry of the discotic nematic liquid crystal. For the wedge disclinations of Figure 2, the rotation vector is parallel to the tangent to the disclination line (core), and for the twist disclinations of Figure 3, the rotation vector is prependicular to the tangent.

The disclinations are classified by the amount of rotation involved and its direction relative to the tangent to the disclination line. The strength of a disclination is a measure of this rotation and is determined by considering the change in the direction of the normals to the disklike molecules about a circuit that encloses the disclination line. The change in local orientation of the normals along the closed curve, a Nabarro circuit [5], is observed. The disclination strength is then defined as the number of revolutions of the direction of the normals with respect to one revolution (2π) about the Nabarro circuit. A Nabarro circuit is illustrated in Figure 4 for a negative wedge disclination of rotation π, that is, a wedge disclination of strength $S = -1/2$. The amount of the rotation of the normals is π, but the rotation is counter (negative) to the direction of the Nabarro circuit.

The crystal defects known as disclinations were conceived many years ago by theoreticians as a part of the general pattern of possible distortions in crystal lattices [6]. Owing to the high lattice distortions involved in

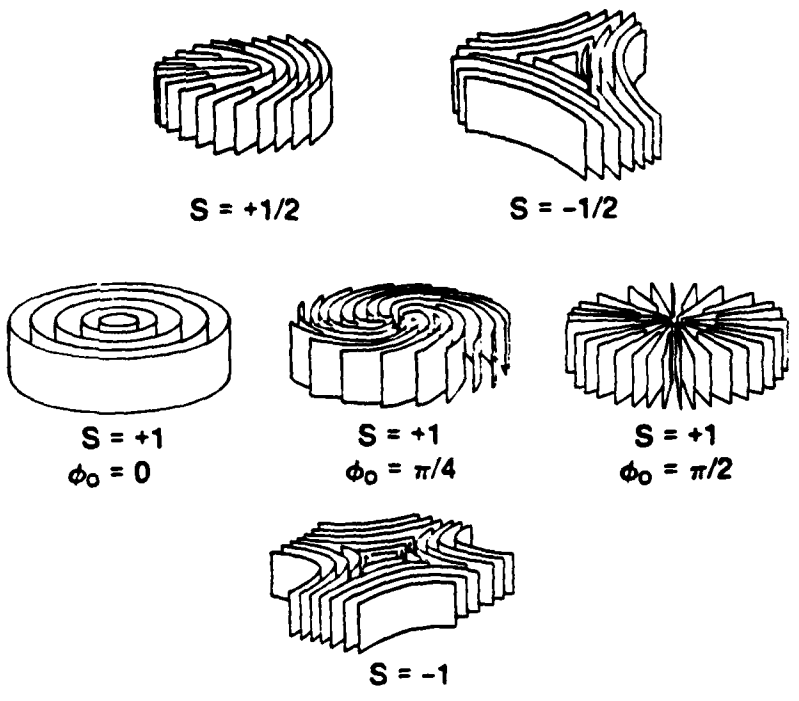

Figure 2. Wedge disclinations in the carbonaceous mesophase. The surfaces denote the layers mapped out by the average direction of the preferred orientation of the individual platelike molecules. The rotation vector is parallel to the tangent to the disclination line.

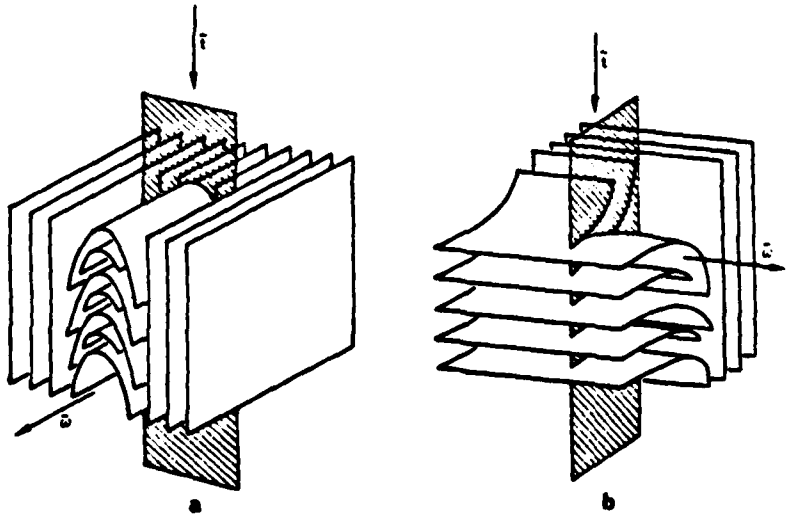

Figure 3. Twist disclinations in the carbonaceous mesophase. The rotation vector is perpendicular to the ribbonlike core.

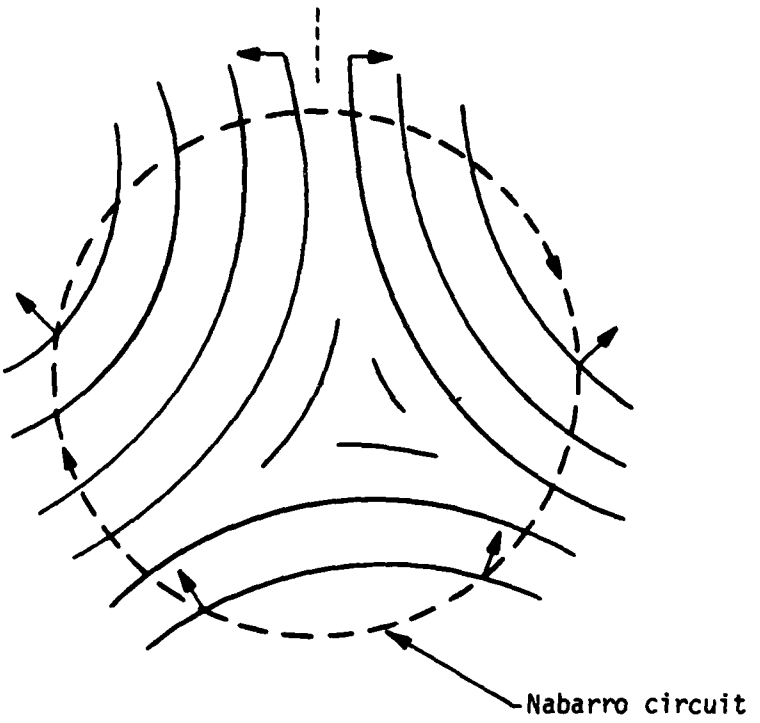

Figure 4. A Nabarro circuit about a wedge disclination. The rotation of the normals is $-\pi$; the strength $S = -\pi/2\pi = -1/2$.

these rotational distortions, it was considered unlikely that disclinations would play a significant role in any structural material. However, disclinations were subsequently found to be prominent features of liquid crystals in which the point-to-point lattice registry between adjacent molecules is not required, thus greatly relaxing the strain fields around the disclination cores. Since the morphologies of carbon-carbon composites are established while the carbonaceous material is in the liquid-crystalline state, the presence of disclinations in these lamelliform morphologies is to be expected. The existence of these layer-stacking defects was demonstrated in 1967, and evidence of wedge and twist disclinations has subsequently accumulated [8, 9].

The presence and types of disclinations is efficiently determined by reflection microscopy with polarized light. The preferred orientation of the mesophase as it intersects a polished plane of section can be defined with cross-polarized light. Crystalline graphite is bifrefringent (optically anisotropic) and thus the reflection of polarized light is dependent on its orientation to the preferred orientation of the mesophase. The reflection contrasts for a graphite single crystal are illustrated in Figure 5. With polarized-light micrography, disclinations are evident as rotation-invariant points in the extinction contours that identify mesophase layers that are perpendicular to a polarizing direction. The disclinations of strength ±1/2 are denoted by a node with two extinction-contour arms. For a rotation of the crossed polarizers, the arms of the S = +1/2 node rotate with the polarizers and the arms of the S = -1/2 node rotate counter to the polarizers. The disclinations of strength S = ±1 are denoted by a cross in the extinction contours -- a point with four extinction-contour arms. The S = +1 disclination is a corotating cross; the S = -1 disclination is a

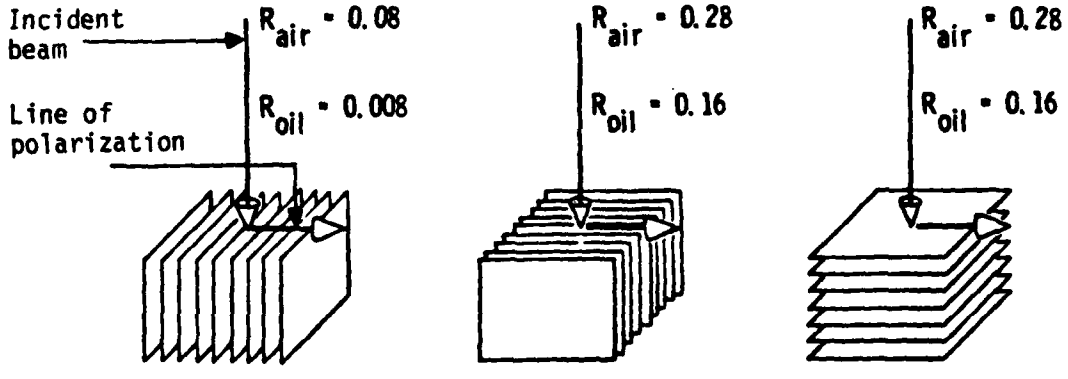

Figure 5. Reflectance of polarized light from a graphite crystal. The differences in reflectance for the carbonaceous mesophase are slightly smaller, but significant to delineate the disclination structures.

counterrotating cross. The polarized-light micrography at various angles of rotation of the polarizers is used to define the molecular orientations about these nodes and crosses in the extinction contours and thus map out the configurations of the underlying disclinations [2].

The identification of the disclinations in the carbonaceous mesophase has been aided by the use of mesophase microconstituents that have a strong preferred orientation. The two microconstituents are the fibrous and lamellar constituents which result from uniaxial and biaxial extension, respectively, of the plastic mesophase. The microconstituents are the needle-like portions of the needle coke and the lamellar bubble walls of voids in the mesophase. These microconstituents have offered good subjects for detailed study because the strong preferred orientation of each microstructure relative to selected planes of section provided the information necessary for resolution of the disclination structures. However, the mesophase which fills the matrix pockets of a multidirectional graphite-fiber preform may not have a distinct preferred orientation, and the array of wedge and twist disclinations may be quite complex.

Another advantage of the carbonaceous mesophase for the study of disclinations is that the mesophase can be quenched to a solid which can be sectioned and studied by optical micrography. Perpendicular planes of section and successive parallel planes of section are used to define the mesophase morphology in three dimensions [10].

Carbon-carbon composites are leading candidate materials for applications that require retention of mechanical properties at high temperature, good thermal-shock resistance, and resistance to chemical erosion. The carbonaceous mesophase plays a key role in the fabrication of these composites, and thus these properties are dependent on the mesophase

morphology formed in each constituent of a carbon-carbon composite. The processing procedures directly control the microstructure of the matrix of the carbon-carbon composites. Densification of these composites involves impregnation with an organic precursor, carbonization and graphitization. Variations include the type of precursor (petroleum pitch, coal-tar pitch, or thermosetting resin), the applied pressure during carbonization, and the graphitization temperature.

The complex, heterogeneous structure of the multidirectional carbon-carbon composites consists of fiber bundles and matrix pockets, each with their own distinct microstructures. Disclinations exist in the matrix within the graphite-fiber bundles and in the matrix regions between fiber bundles. Each has its characteristic disclination structure and thus may play a different role in the relation of disclinations to the properties of the carbon-carbon composites.

DISCLINATION ARRAYS

An understanding of disclination arrays in the carbonaceous mesophase is necessary to define the basic microstructure of the matrix of a carbon-carbon composite. Disclinations are not isolated distortions in the matrix but exist in great numbers and can be as close together as 5 to 10 microns. Examples of the disclination arrays are shown in Figures 6 and 7. These optical micrographs show the extinction contours that indicate those regions of the underlying microstructure that are perpendicular to the crossed polarizers. The nodes, where the extinction contours pinch down to a point, denote disclinations of strength $S = \pm 1/2$ and the crosses in the extinction contours denote disclinations of strength $S = \pm 1$. The sample is Ashland A240 petroleum pitch heated at 400°C for 24 hrs. This pyrolysis cycle was designed to provide coarse mesophase without much deformation by bubble percolation. All optical micrographs in this report were taken with a Neophot 21 reflected-light microscope (Zeiss aus Jena).

These micrographs show that there tends to be more of the disclinations of lower strength. The energy of a disclination [11] is

$$E = \pi K S^2 \ln \frac{R}{r_o} + E_{core} \qquad (1)$$

where E is the elastic energy per unit length of the disclination line, R is the size of the sample or the distance between neighboring disclinations, r_o is the radius of the core of the disclination and S is its strength. The

disclinations of strength ±1/2 have one-fourth of the energy of the disclinations of strength ±1. The strain energy of an unlike pair of disclinations is

$$E_p = -2\pi KS^2 \ln \frac{d}{r_o} \qquad (2)$$

where d is the distance between disclinations [12]. The energy of a like pair is positive. Thus, to minimize the total energy of an array, neighboring disclinations of opposite sign will occur about as often as neighboring disclinations of the same sign.

The molecular arrangement underlying the pattern of extinction contours is shown in Figure 8. A series of micrographs at various rotations of the cross polarizers were made and, by the use of an overlay, the orientation of the layers in the mesophase was sketched at each rotation. These disclination arrays are probably introduced by the coalescence of mesophase spherules that are oriented randomly with respect to each other and to the surface of the bulk mesophase. The mesophase has fluidity such that rearrangement of the disklike molecules can occur and the disclination arrays can adjust to a minimum energy configuration.

Work to be continued in this area includes defining the three-dimensional morphology of these disclination arrays. On single plane of section, the types of disclinations can be determined from the polarized-light micrography and the location of the intersection of the disclination line with the plane of section. The direction of the tangent to the disclination line is required to determine if a disclination is pure wedge or twist or if it is a mixed disclination with both wedge and twist character [10]. The three-dimensional morphology will be determined by observation of a specific area on successive planes of section which are a few microns apart. Thus, the direction and curvature of the disclination lines can be determined.

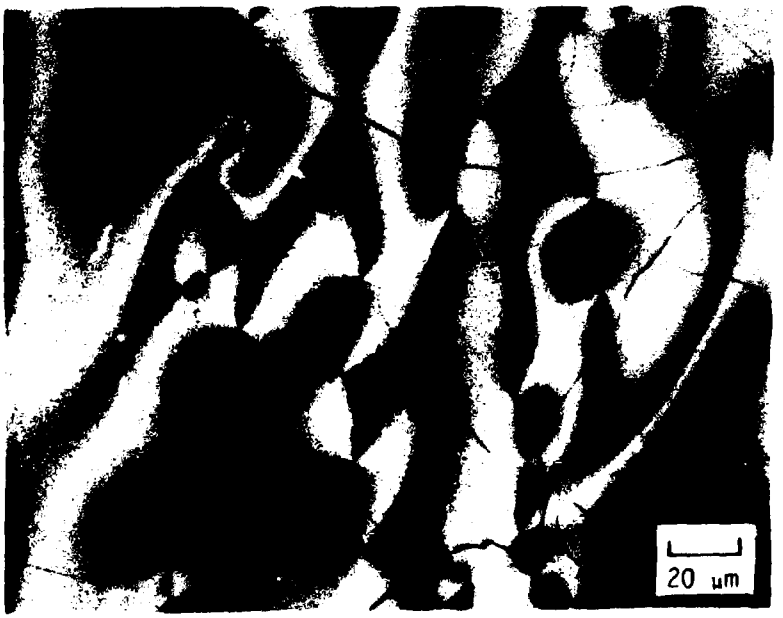

Figure 6. Optical micrograph of disclination array in coarse mesophase. There are 13 S = -1/2 and 13 S = +1/2 disclinations, cross polarizers.

Figure 7. Optical micrograph of disclination array in coarse mesophase. There are 13 S = +1/2, 9 S = -1/2, 3 S = +1 and 3 S = -1 disclinations, cross polarizers.

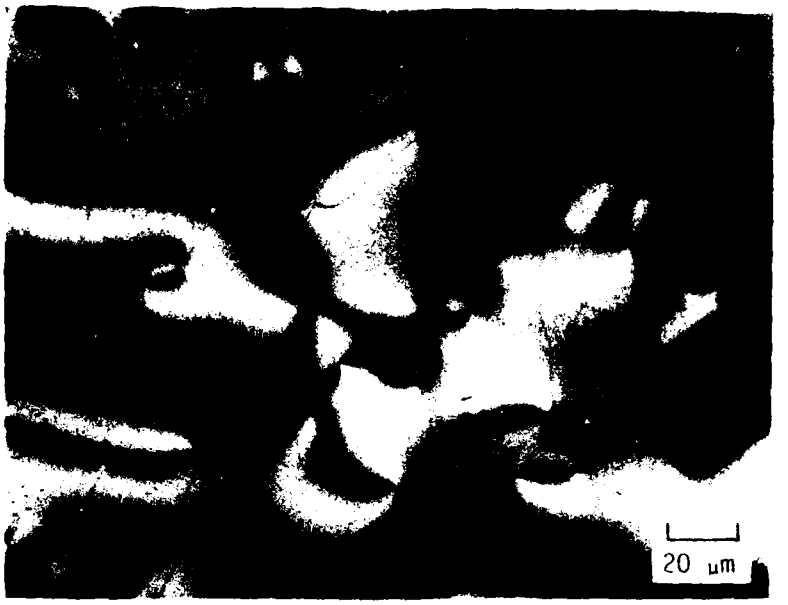

Figure 8. Optical micrograph and structural sketch of disclination array.

DISCLINATIONS AND FRACTURE

One of the properties of graphitic materials that is expected to be affected by disclinations is fracture toughness. Cracks in graphitic materials propagate preferentially parallel to the basal planes in directions approximately normal to the applied stress. When a cleavage crack attempts to follow a basal layer in a complex structure with curved layers, it can become diverted to a nonpropagating direction by the bends, folds, and discontinuities present [13, 14]. Multiple fracturing and fracture normal to basal planes often occurs, and thus, graphites have a high work of fracture as compared to most ceramic materials (Figure 9). This present research is aimed at determining the relationship between fracture and the disclination structures in the carbonaceous mesophase, the matrix constituent of carbon-carbon composites.

Crack propagation in the carbonaceous mesophase has been studied with the use of optical micrography. Polished, thin sections (1 to 2 mm) of mesophase coke were bonded to a wedge-opening graphite specimen designed to produce incremental crack growth (Figure 10). The cracks were photographed after each segment of crack propagation. From micrographs taken with cross-polarized light at various rotations of the polarizers, the mesophase microstructure about each crack segment was determined. The mesophase coke was prepared by pyrolysis of A240 petroleum pitch at 400°C for 24 hr, removal

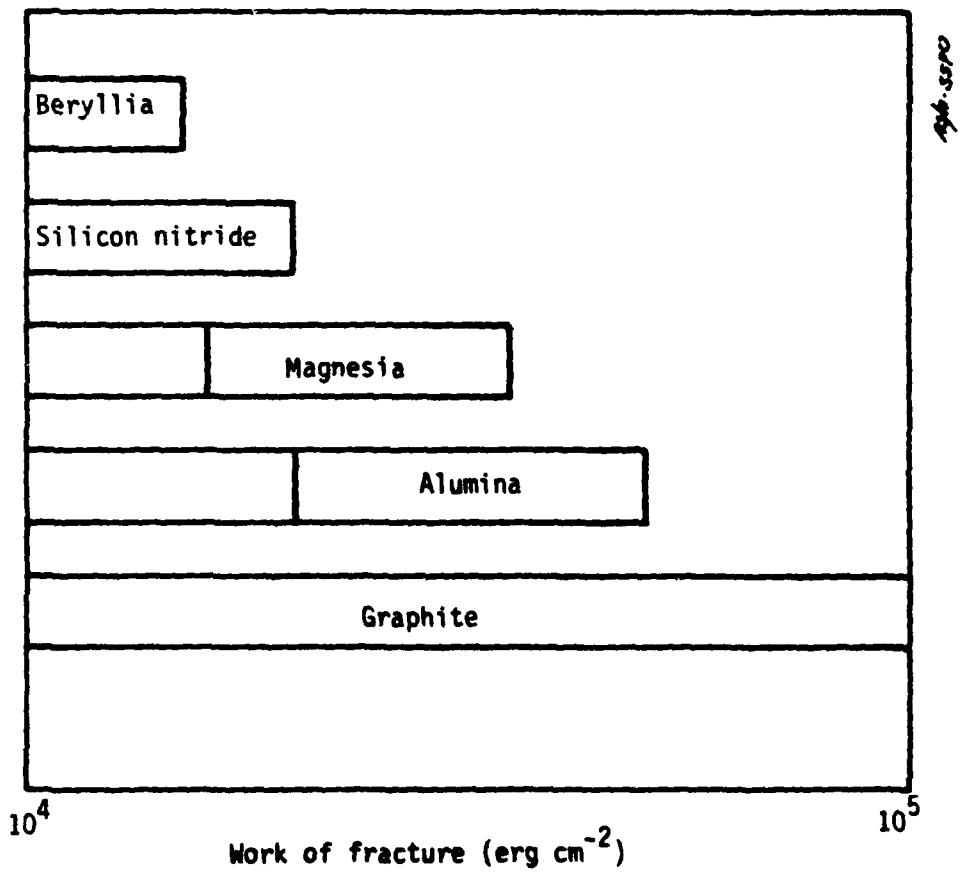

Figure 9. Fracture toughness of polycrystalline ceramics [15].

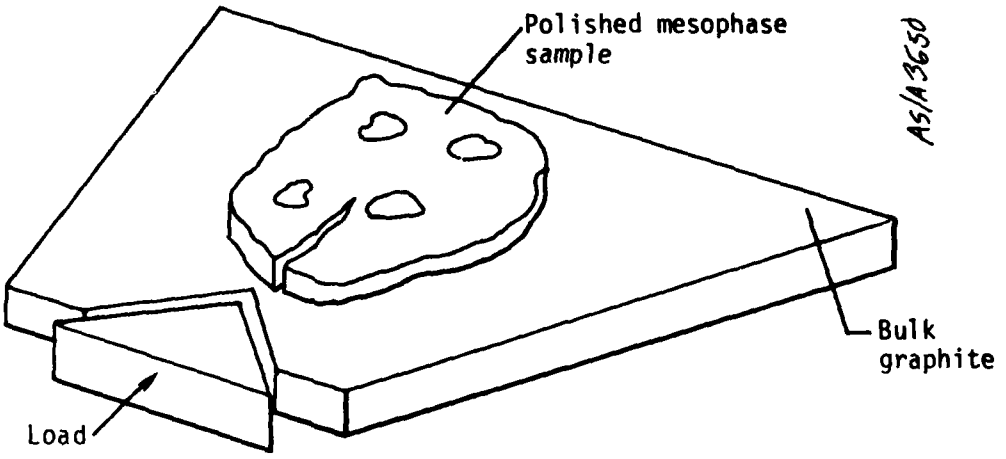

Figure 10. Fixture for crack propagation studies.

of remaining volatiles at 300°C in vacuum, and subsequent heat treatment to 600°C. This coke had a coarse, undeformed structure for easy identification of the disclinations present. At this level of heat treatment, some crack propagation across the mesophase layers occurred. Heat treatment to graphitization temperatures would help assure crack propagation by cleavage, but the optical response of such a sample is masked by extensive shrinkage cracks. Thus the mesophase coke heat treated to 600°C was found to provide clearer evidence of the effect of disclinations on crack propagation.

Sketches of the crack path and the adjacent disclination structures are shown in Figures 11 though 14. The cracks tended to follow the basal layers, but some cracking normal to the layers occurred. This is probably a result of the crack path at the surface being controlled more by the crack path in depth in the sample. The curvature associated with the disclinations produced a jagged crack path, as shown in Figure 11. In Figure 12, the crack was forced to go around a disclination of strength S = +1/2. The crack appears to have

been stopped by a disclination of strength S = +1/2 in Figure 13. At a disclination of strength S = -1/2 in Figure 14, the crack was diverted into two crack branches. Disclinations of strength ±1 also affected the crack path. Thus, this evidence indicates in a qualitative way that the disclinations present in the microstructure of graphitic materials contribute to crack blunting, crack diverting, and energy absorption, which result in the high work of fracture.

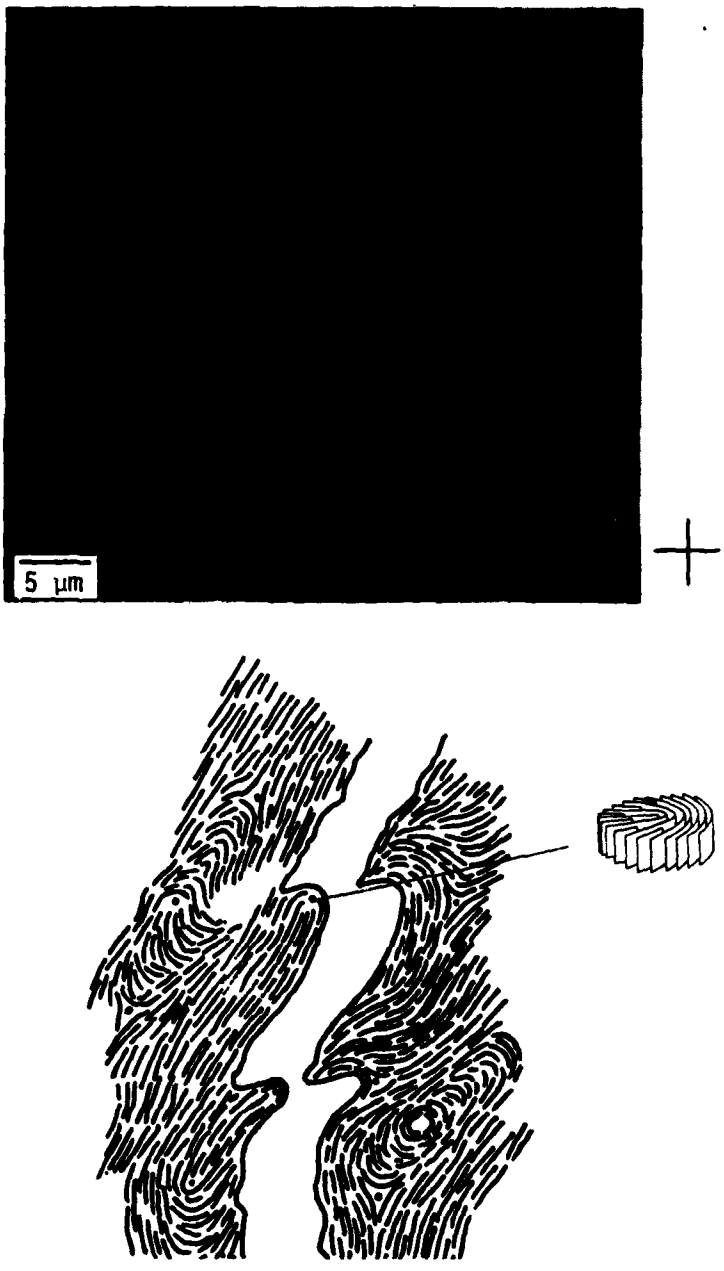

Figure 11. Crack path controlled by basal-plane curvature and disclinations.

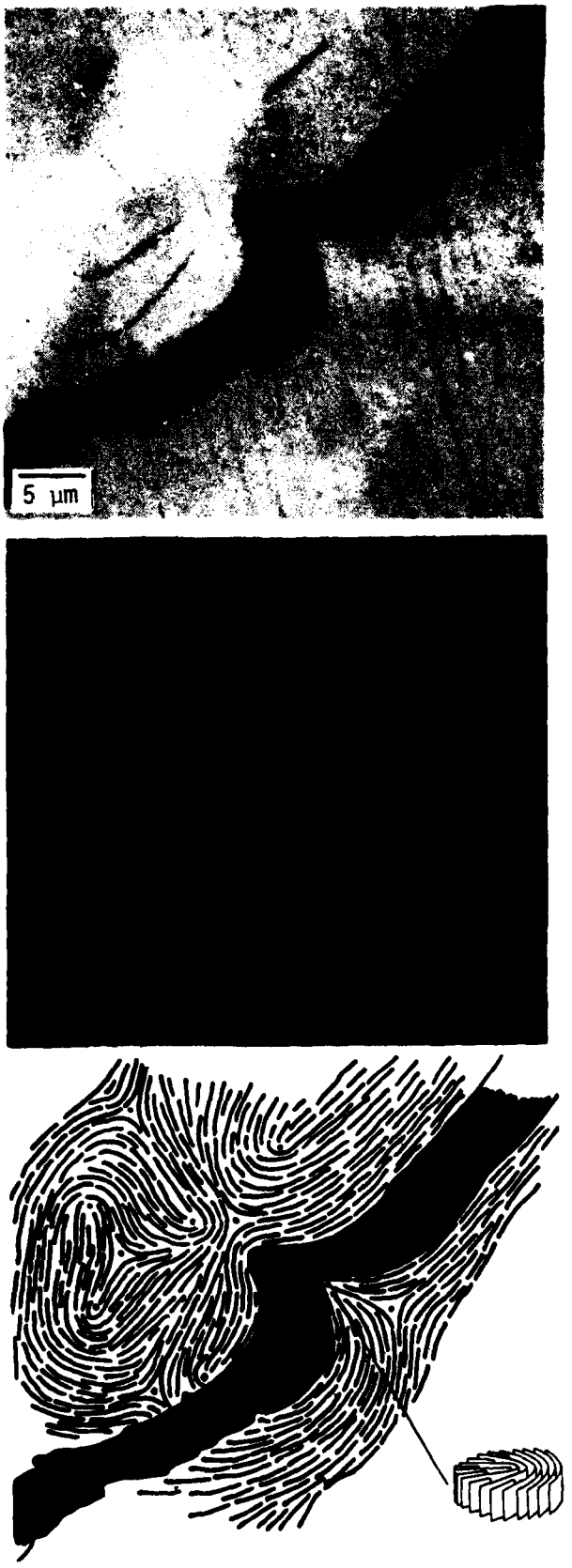

Figure 12. Crack path diverted by S = +1/2 disclination.

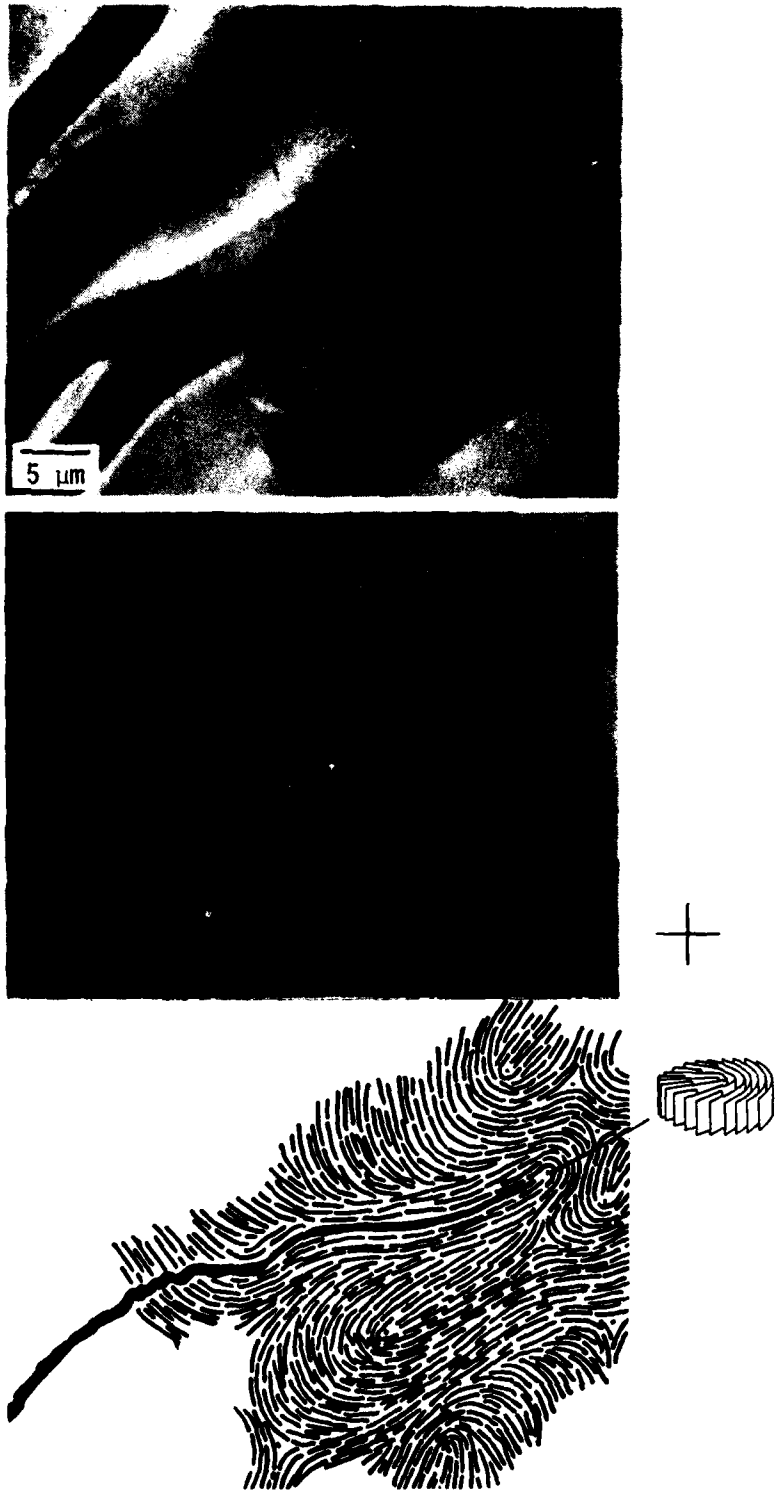

Figure 13. Crack blunting at disclination of strength S = +1/2.

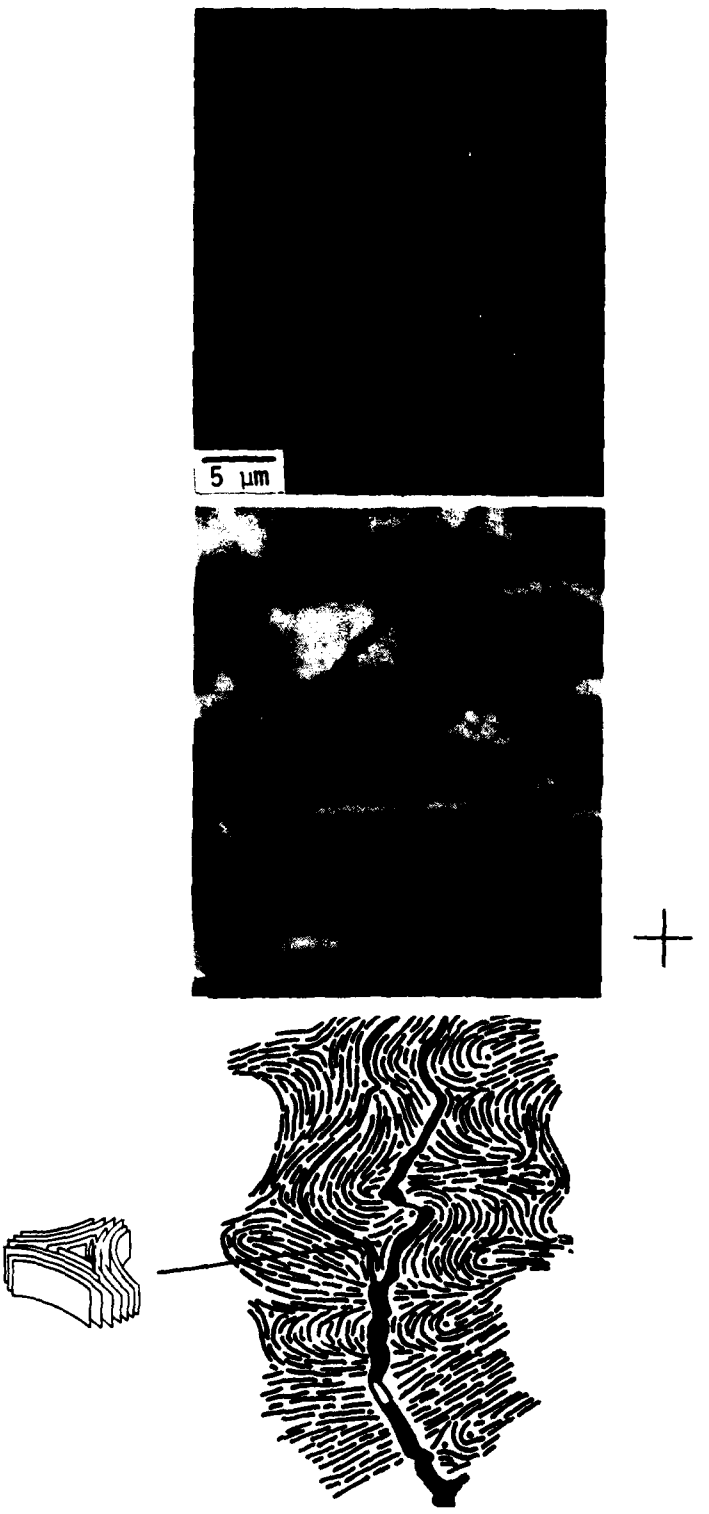

Figure 14. Crack branching at disclination of strength S = -1/2.

DISCLINATIONS IN A FIBER BUNDLE

In a carbon-carbon composite, the graphite filaments are typically aligned parallel as fiber bundles consisting of thousands of the filaments which are about 7 microns in diameter. Among these graphite filaments from rayon, polyacrylonitrile, or mesophase pitch is the graphite matrix formed via the carbonaceous mesophase. In this matrix among the graphite filaments are disclinations. Three major aspects of the disclinations in a fiber bundle are described here: the orientation of the filaments and the alignment of the mesophase by the filaments defines the type of disclination present; the arrangement of the filaments prescribes the strength of the disclinations; and first evidence is presented for the existence of disclinations of strength greater than 1.

The specimen prepared for this study of the disclinations in a fiber bundle contained graphite filaments in mesophase formed from Ashland A240 petroleum pitch. The filaments were Hercules HM 1000 filaments fabricated from a polyacrylonitrile precursor. Yarns of 1,000 filaments were aligned parallel in a graphite frame with a spacing between the bundles of about 5 mm. The bundles were vacuum impregnated with A240 pitch and then carbonized at 400°C for 24 hr at atmospheric pressure in nitrogen. This carbonization cycle was designed to provide a mesophase microstructure free of excessive

deformation from bubble percolation. The sample was sectioned perpendicular to the fiber bundles and polished for optical microscopy.

Negative Wedge Disclinations

The disklike molecules of the carbonaceous mesophase prefer to align parallel to the surface of the graphite filaments. This tendency for the molecules of the mesophase to align parallel to substrate surfaces has been shown for graphite flakes, coke particles, and ceramic materials [16,17]. The parallel alignment about the graphite filaments is shown in Figure 15. This micrograph shows several of the round, graphite filaments and the surrounding matrix. The structural sketch was made by tracing on an overlay on the micrograph the orientation of the mesophase layers underlying the extinction contours. This was done for micrographs at various angles of rotation of the crossed polarizers (not shown) to map out the entire matrix region. The parallel alignment results in a circular sheath about each filament. This sheath is several microns in thickness and extends the length of each filament.

Within a fiber bundle, the alignment of the mesophase as a circular sheath about the filaments prescribes the morphology of the remaining volume of matrix. Evident among the filaments are disclinations: those points where the parallel stacking of the mesophase layers is interrupted. These are wedge disclinations. The parallel alignment of the filaments and mesophase sheath force the disclination lines to be parallel to the filaments. The rotation vector for these disclinations is parallel to the disclination line and thus these disclinations are pure wedge disclinations.

Each sheath effectively constitutes a positive wedge disclination of strength $S = +1$. As shown previously for the disclination arrays in the carbonaceous mesophase, there must be a balance of disclination strengths to

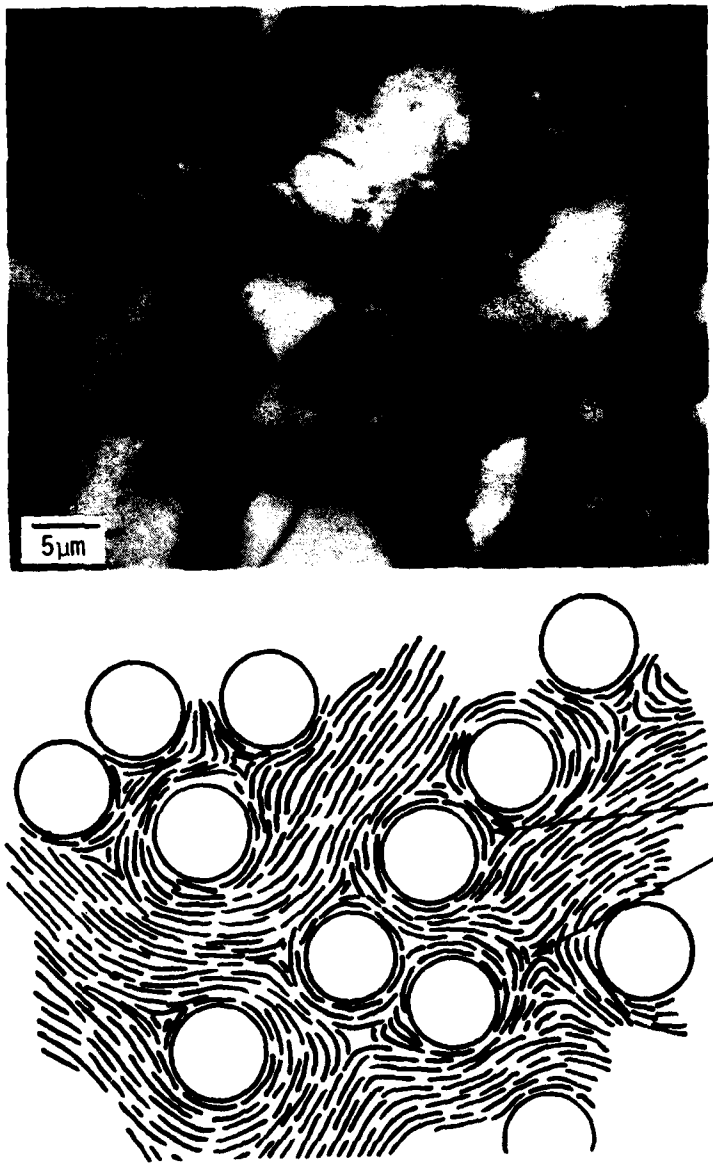

Figure 15. Micrograph and structural sketch of matrix among graphite filaments in fiber bundle. The mesophase aligns in a circular sheath about each filament.

minimize the total disclination energy (and to minimize any net torque of the material). Thus, the matrix among the sheaths of positive strength must contain predominately negative wedge disclinations. This is the case for Figure 15 (cf. Figure 2). For an array of parallel filaments, the sum of the strengths of the sheaths and the negative wedge disclinations tends to zero.

Disclinations of Strength -1/2 and -1

The strengths of the negative wedge disclinations are determined by the local arrangement of the filaments. For closely packed filaments in a triangular array, the enclosed disclination has strength S = -1/2, as shown in Figure 16. For filaments in a square array, the enclosed disclination has strength S = -1, as shown in Figures 17 and 18. A square array and a triangular array in proximity are shown in Figure 19. These representative micrographs indicate that the type and character of the disclinations in a fiber bundle are prescribed by the alignment of the mesophase matrix by the filament surfaces and the pattern of the filament arrays.

These disclinations of strength S = -1/2 and -1 are common in bulk mesophase without filaments, as well as the disclinations of strength +1/2 and +1. In the fiber bundle, however, their geometry is more defined. The disclination lines tend to be straight and parallel, where in the bulk mesophase they may be curved.

Disclinations of Strength -3/2 and -2

The fiber bundle provides a background structure that governs the strength of the negative wedge disclination. Disclinations of higher strength, not commonly found in bulk mesophase, may be expected to exist in certain arrays of filaments. The relation between the type of array and the disclination strength is given in Table 1.

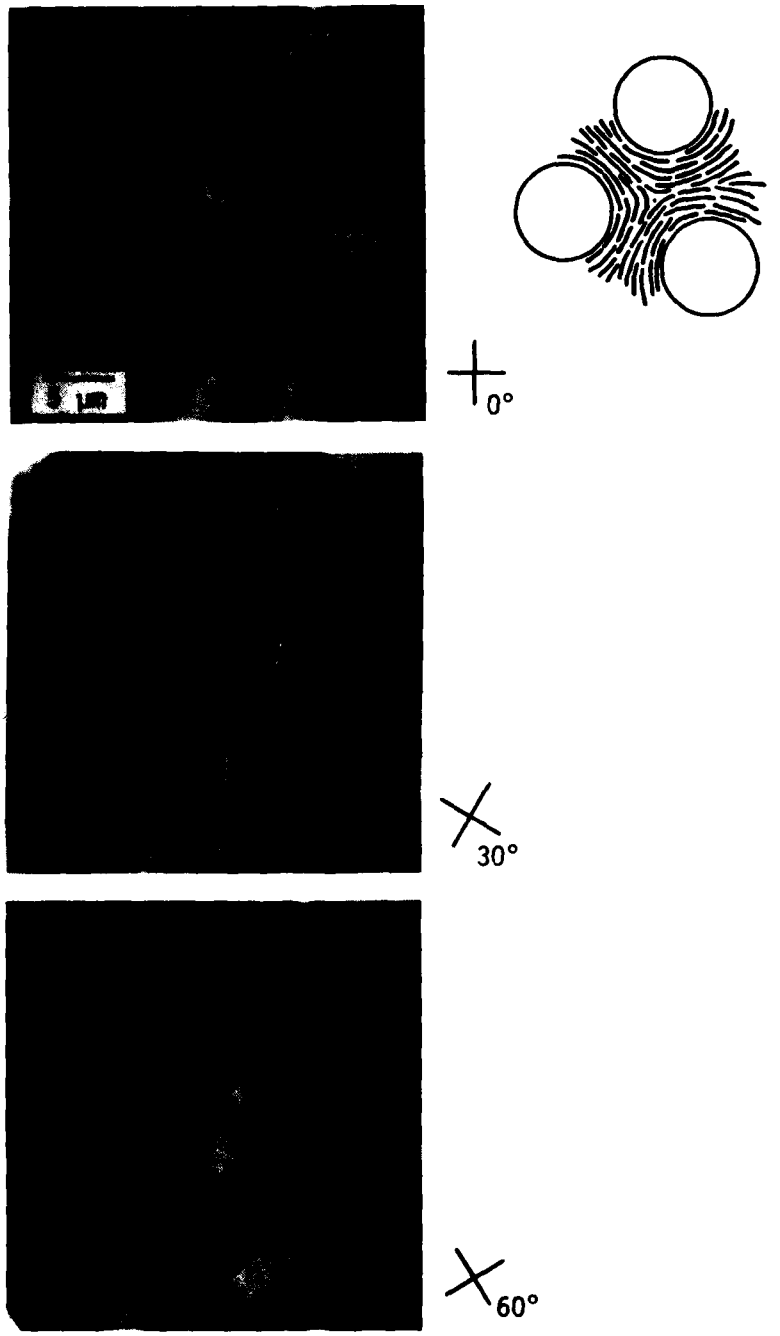

Figure 16. Disclination of strength S = -1/2 in a triangular array of graphite filaments. Crossed polarized light with immersion oil.

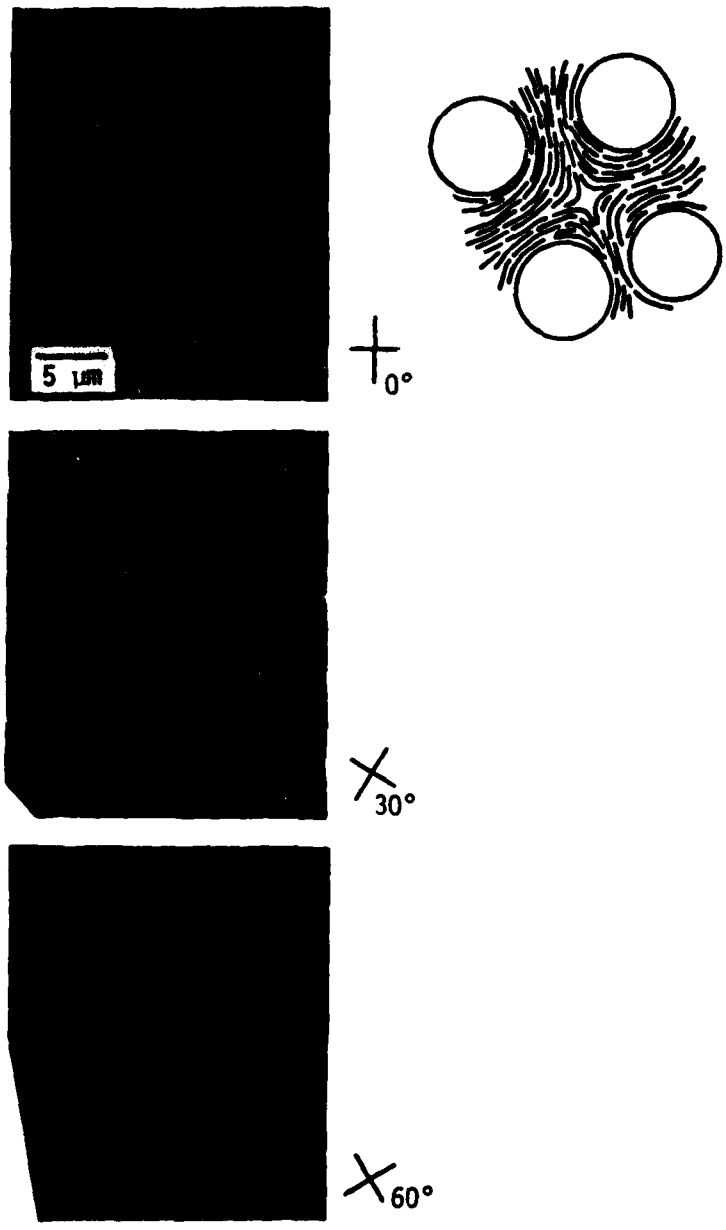

Figure 17. Disclination of strength S = -1 in a square array of graphite filaments.

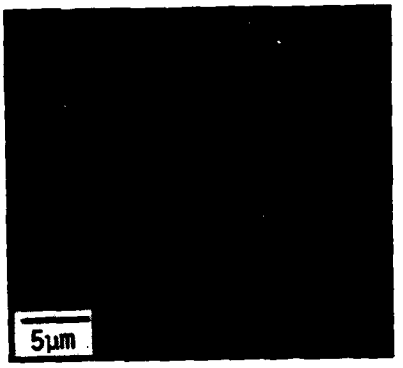

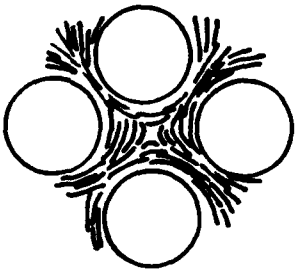

Figure 18. Square array with S = -1 disclination.

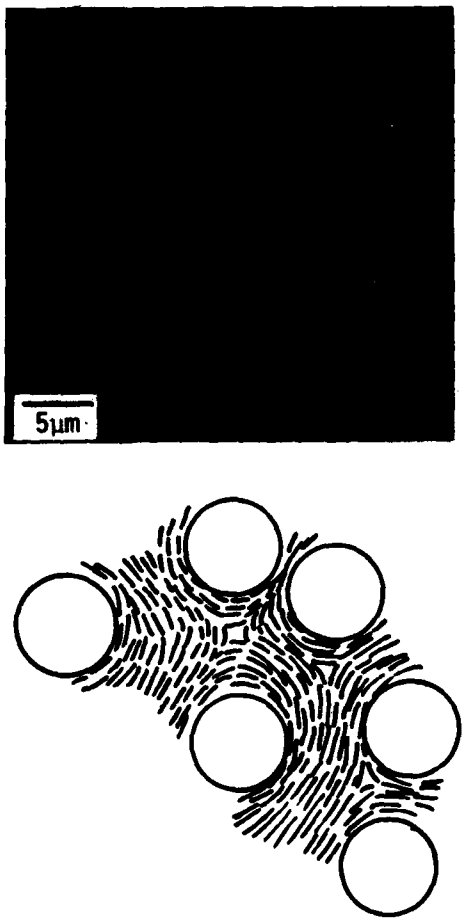

Figure 19. Two triangular arrays with S = -1/2 disclinations and one square array with an S = -1 disclination.

Table 1. Disclinations in Filament Arrays

Array	Strength of Disclination	Number of Extinction-Contour Arms	Core Structure	Relative Energy
Triangular	-1/2	2	Discontinuous	1
Square	-1	4	Continuous	4
Pentagonal	-3/2	6	Discontinuous	9
Hexagonal	-2	8	Continuous	16

Thus, a disclination of strength S = -3/2 should exist in a pentagonal array and could be identified by its six extinction-contour arms. Similarly, in a hexagonal array, a disclination of strength S = -2 should have eight extinction-contour arms.

An apparent disclination of strength S = -3/2 is shown in Figure 20, along with a structural sketch showing the configuration of this disclination. The central region, or core of the disclination, is not sketched, as the resolution of the optical microscope is limited to about 1μm, the size of this core. The core structure of the negative wedge disclinations will be described in detail in the following section.

For the pentagonal array of Figure 21, there is no disclination of strength S =- 3/2, but two disclinations of strength S = -1/2 and S=-1. The energy of the disclination is related to the square of its strength [11] and thus in this case, the mesophase has realigned by viscous flow during the liquid-crystal stage to th's lower energy configuration. Thus the presence of a S = -3/2 disclination in a pentagonal array is not assured, but is likely. Few pentagonal (and hexagonal) arrays occur in a typical fiber bundle.

Disclinations of strength S = -2 in hexagonal filament arrays are shown in Figures 22 to 24. The disclination is indicated by its eight extinction-contour arms and a broad, undefined core region. In these cases, the presence of the seventh filament results in an adjacent, second disclination. Figure 25 shows a hexagonal array without an S = -2 disclination, but with an S = -1 and two S = -1/2 disclinations.

To the authors' knowledge, this is the first evidence reported of disclinations of strength higher than 1. Their existence is made possible only by the unique arrangement of graphite filaments and the alignment of the carbonaceous mesophase about the filaments.

Core Structure of Wedge Disclinations

The wedge disclinations in the carbonaceous mesophase are discontinuities in the parallel stacking of the disklike molecules of this liquid crystal. Along the disclination line or core of the disclination, this parallel stacking is not retained and a distinct discontinuity should exist in the core. This core structure is different for each type of disclination and thus an understanding of their core structures should aid in identifying the disclinations and add support to the evidence of their existence. Presented here are a description of the core structure of the disclinations of strength S = ±1/2 and S = ±1, some evidence of the core structure for the disclinations of strength S = -2 and an analysis of the core structures by mapping of the layer orientations in the core region.

Background

The core structures of the disclinations of strength S = ±1/2 and S = ±1 in conventional nematic liquid crystals with rodlike molecules have been extensively studied [18-23]. These studies have shown that the disclinations of strength S = ±1/2 have discontinuous cores and that the core

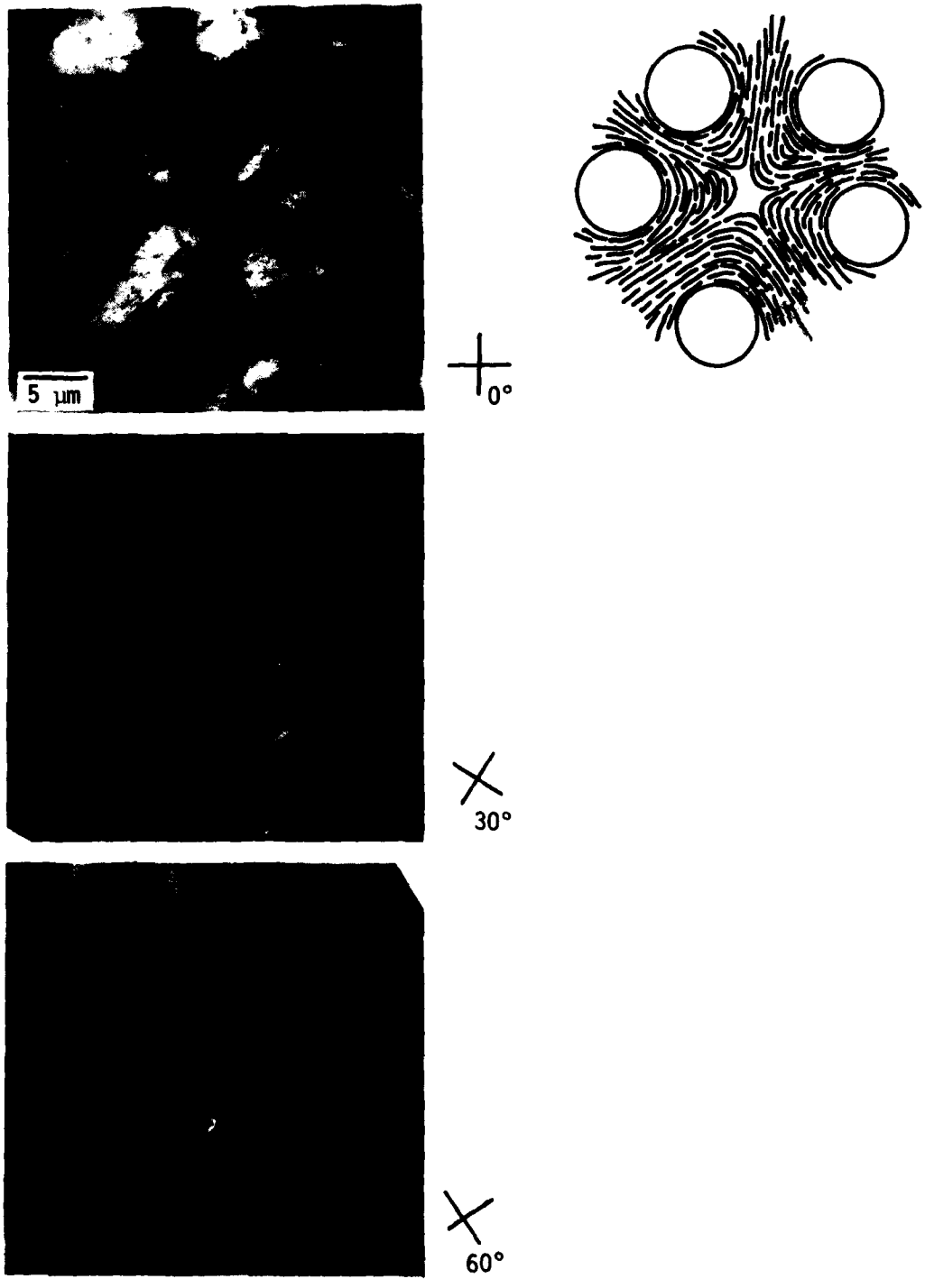

Figure 20. Pentagonal array of graphite filaments with nonrotating point with six extinction-contour arms. This suggests a wedge disclination of strength S = -3/2.

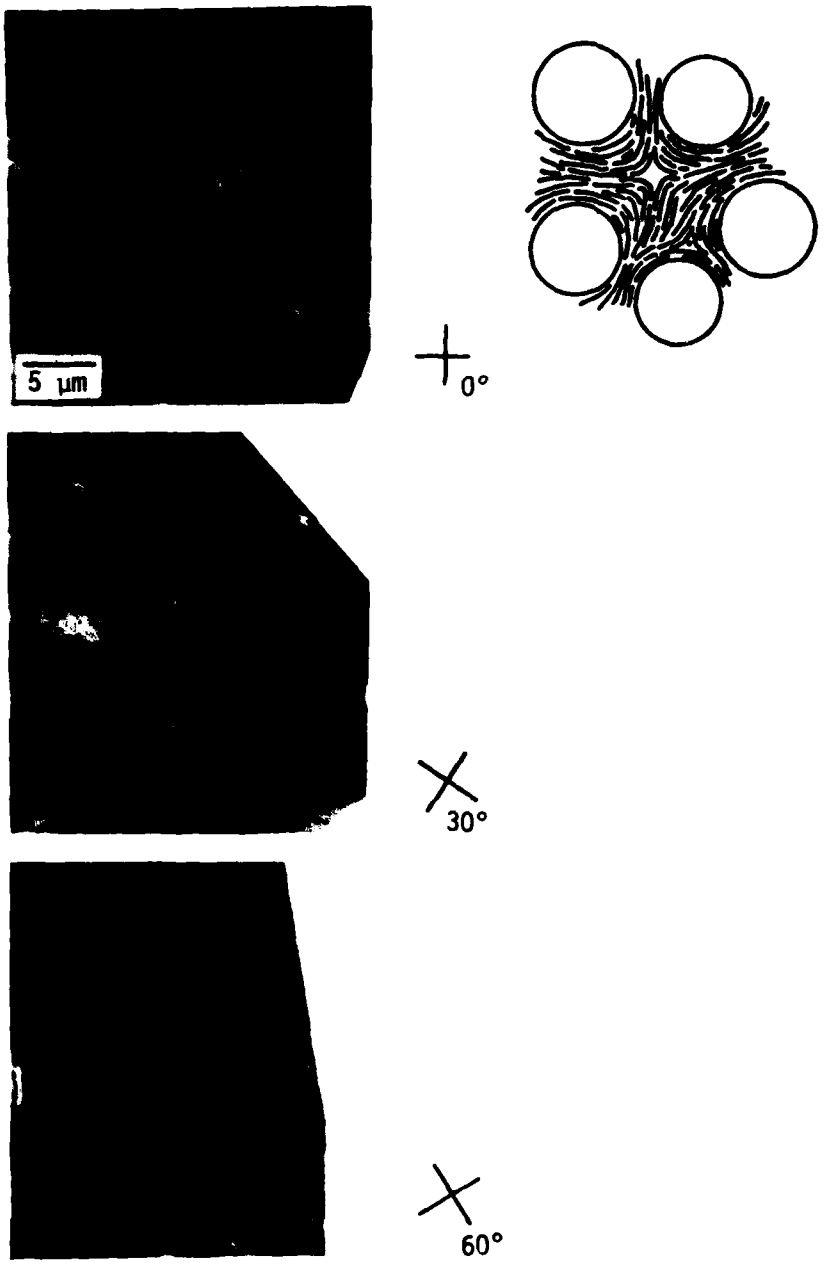

Figure 21. A pentagonal array without an S = -3/2 disclination, but with an S = -1 and an S = -1/2 disclination.

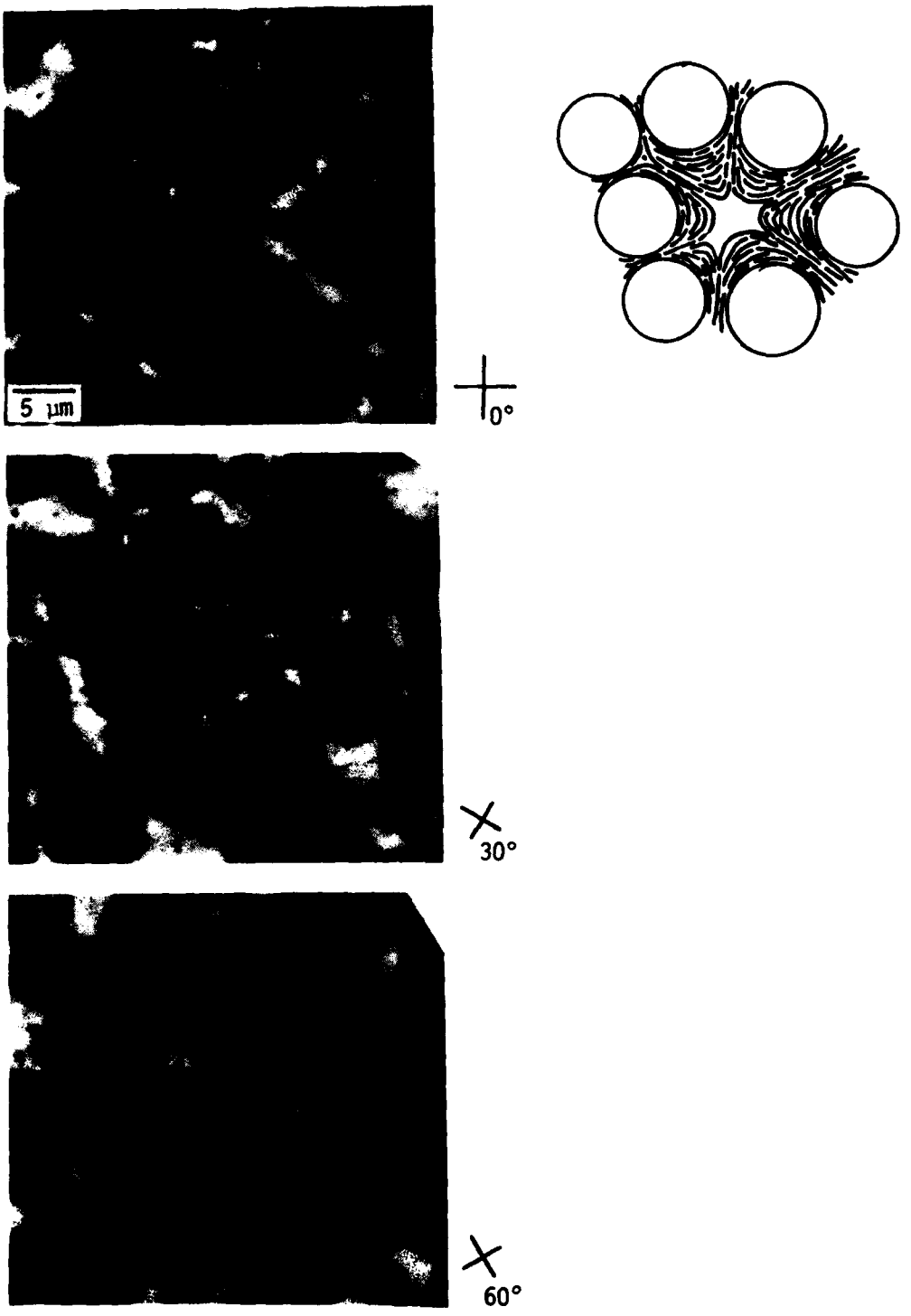

Figure 22. A wedge disclination of strength S = -2 with eight extinction-contour arms in a hexagonal array of graphite filaments.

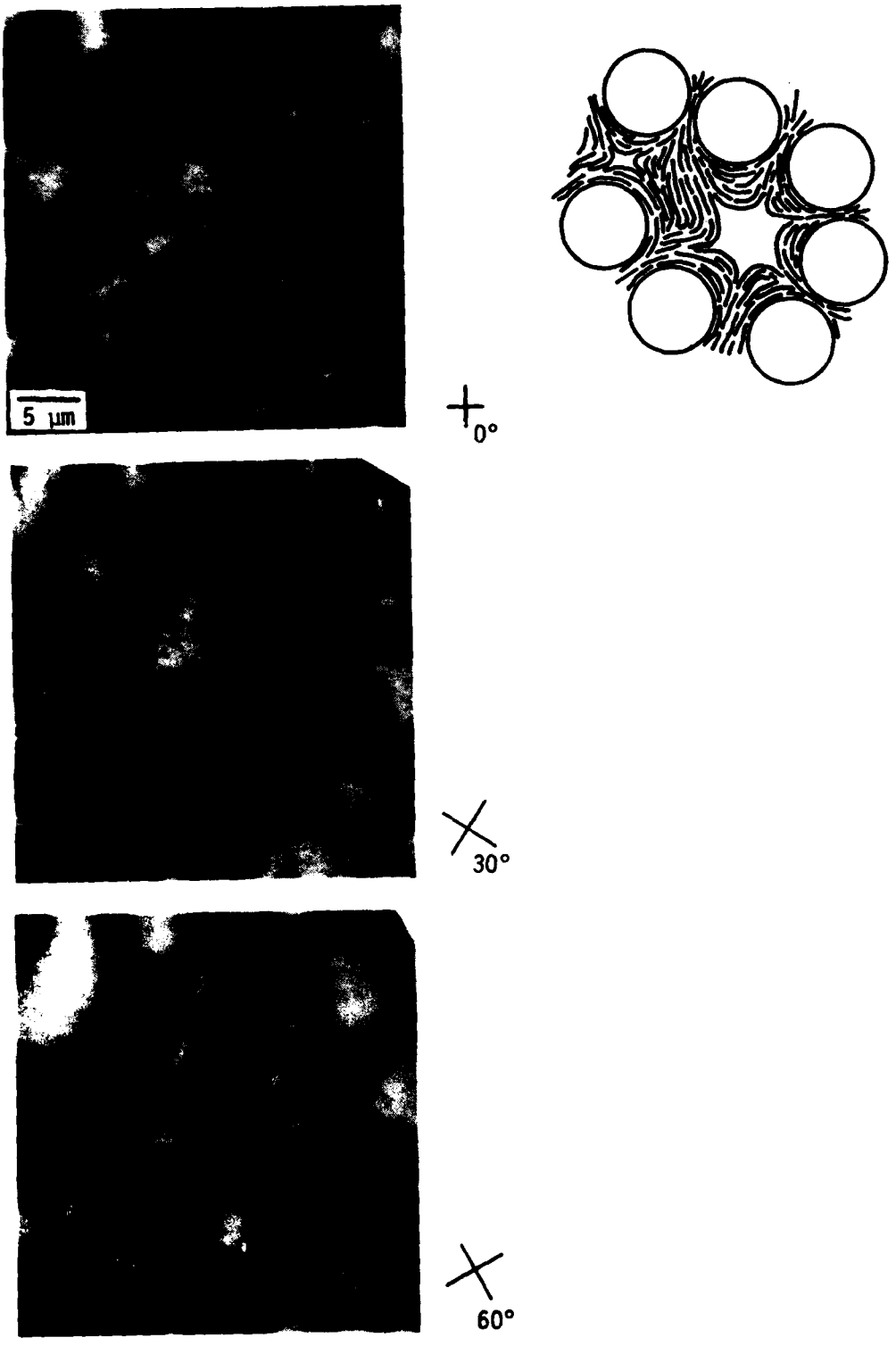

Figure 23. An S = -2 disclination in a hexagonal array.

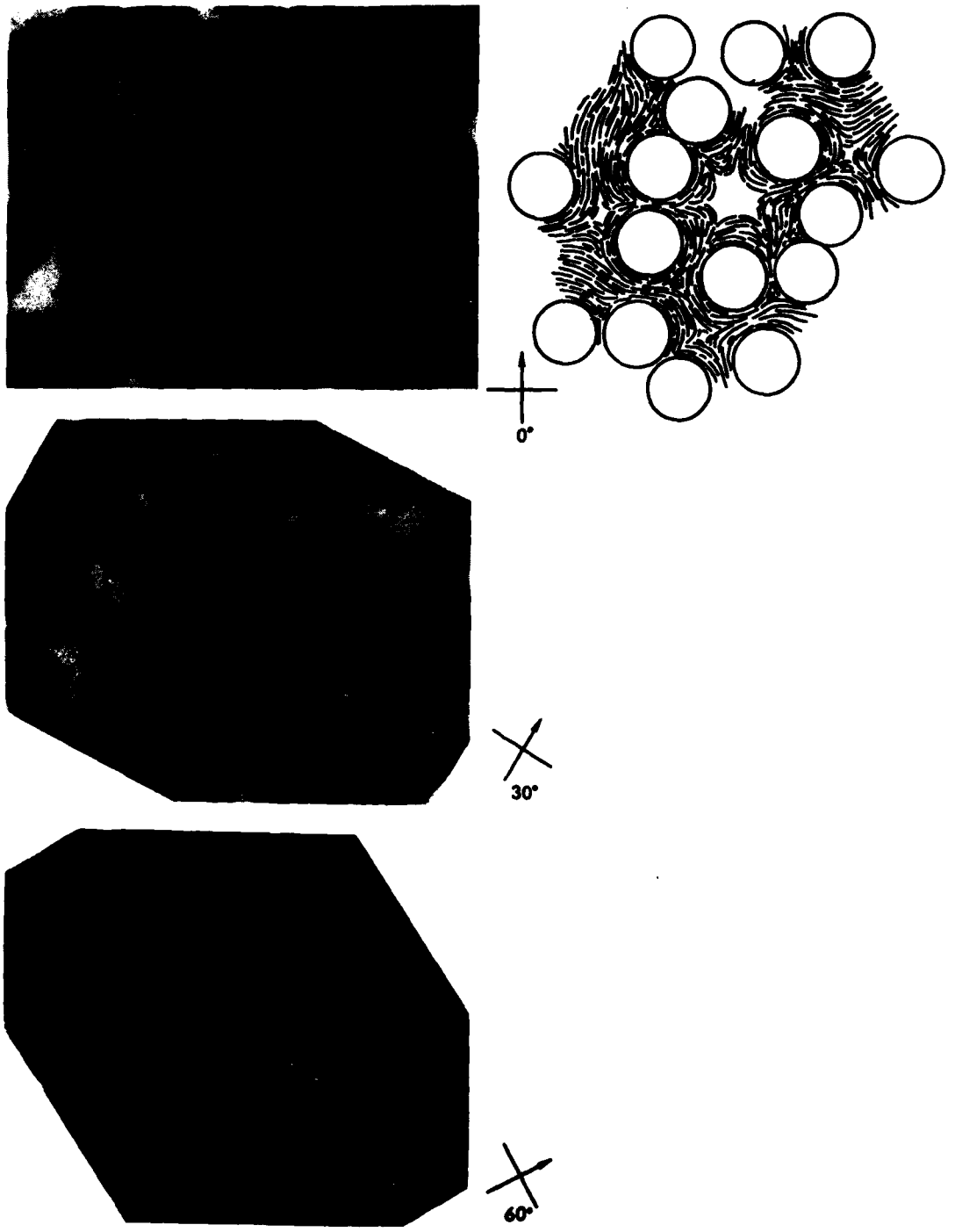

Figure 24. An S = -2 disclination in a hexagonal array.

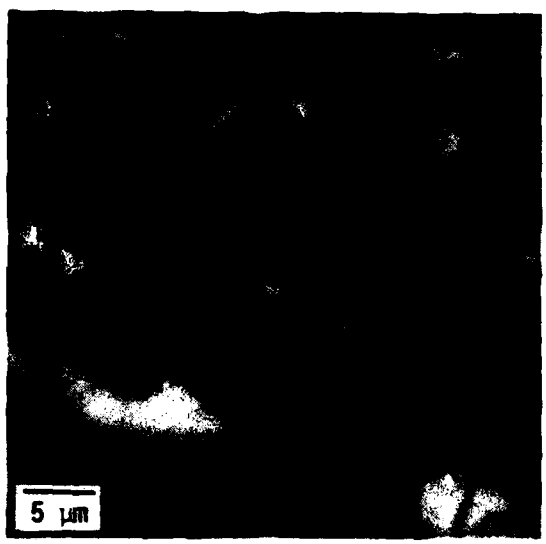

Figure 25. A hexagonal array without an S = -2 disclination. There are two S = -1/2 and one S = -1 disclinations.

must be a line. In a discontinuous core, the configuration of the molecules on the plane perpendicular to the disclination line is retained to the center of the disclination. The core region is of molecular dimensions and consists of a few molecules not in proper alignment. The disclinations of strength $S = \pm 1$ have continuous cores. Continuous refers to the condition where the parallel alignment of the molecules (rodlike or disklike) is retained throughout the core by tilting of the molecules out of the plane of the disclination which is perpendicular to the disclination line. For conventional nematic liquid crystals observed between two cover glasses, the $S = \pm 1$ disclinations are point disclinations. However, by proper sample geometry, such as a capillary tube, the $S = \pm 1$ disclinations can be line disclinations with a continuous core structure.

The core structure of the $S = \pm 1/2$ and $S = \pm 1$ disclinations in the carbonaceous mesophase has been presented previously [24]. The nature of the core of these disclinations is evident in the polarized-light micrographs. The node of the $S = \pm 1/2$ disclinations with the discontinuous cores pinches down to a point (Figure 19) whereas the cross of the $S = \pm 1$ disclinations with the continuous cores has a broad, undefined center. The continuous core has a dimension much larger than the molecule dimensions. The change in layer orientation in this core cannot be resolved by the optical micrography and thus the extinction-contour cross has the broad central point.

The core structure of the disclination of strength $S = +1$ consists of the molecular layers oriented in the shape of a cup, as shown in Figure 26. The core structure of the disclination of strength $S = -1$ is saddle-shaped, as shown in Figure 27, along with a disclination of strength $S = -1/2$ with a discontinuous core, as they exist in an array of filaments.

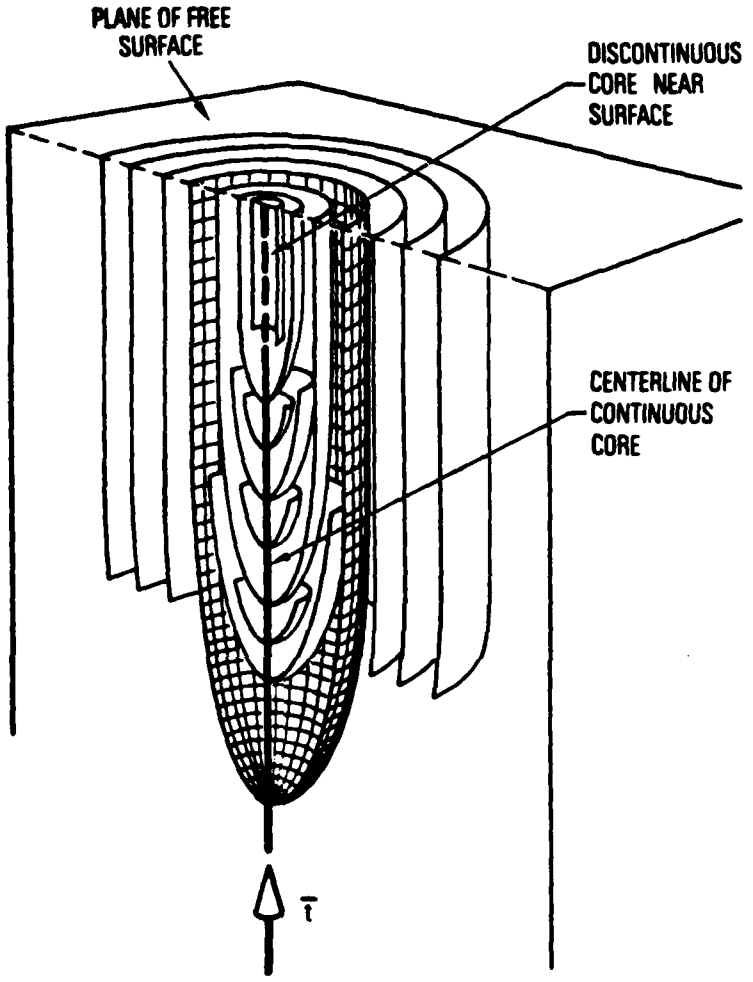

Figure 26. Model of an S = +1 wedge disclination. The grid on one surface defined by the layer orientations shows the cup-shaped structure of the continuous core. The core becomes discontinuous at the intersection with a free surface.

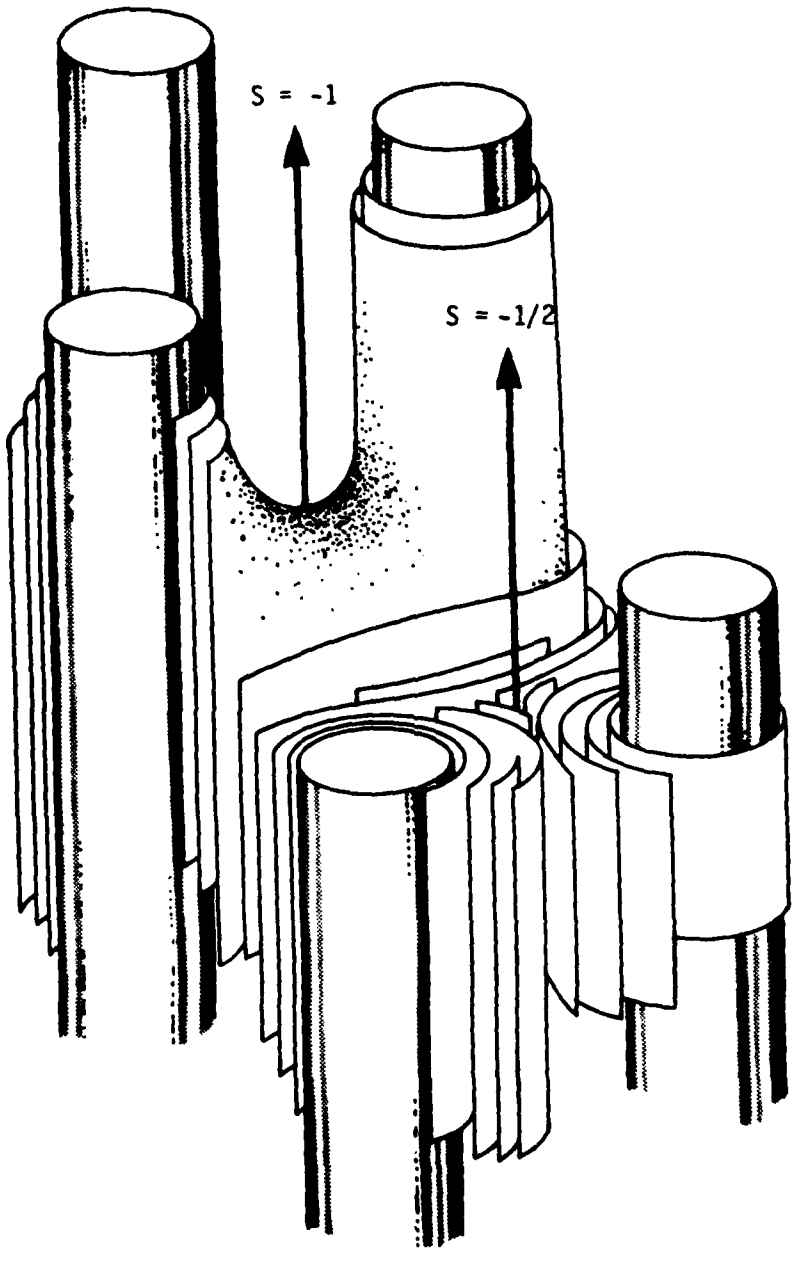

Figure 27. Saddle-shaped structure of the continuous core of an S = -1 wedge disclination in a filament array. Also shown is an S = -1/2 wedge disclination with its discontinuous core.

Evidence of Core Structure

On a plane of section perpendicular to the filaments in a fiber bundle and the associated wedge disclinations, most of the mesophase layers will lie nearly perpendicular to the plane of section. However, a unique feature of the S = -1 disclinations is that in the core region, there are layers that lie parallel to the plane of section (perpendicular to the filaments). The reflection contrast for the layers parallel to the plane of section aids in the identification that a disclination has a continuous core.

The upper left micrograph of Figure 28 shows a region of a fiber bundle under bright field conditions. The center of each cross (S = -1 disclination) in the micrograph with cross-polarized light appears as a bright spot in the bright-field micrograph. Referring to Figure 5, layers which are perpendicular to the plane of section reflect only those electric vectors of the unpolarized light that are parallel to the layers. For the layers parallel to the plane of section, all the electric vectors of the unpolarized light are reflected and thus this core region appears brighter. The micrographs with single polarizers show that the layers about the central spot are oriented nearly perpendicular to the surface but do not overlap the core region.

Bright-field micrographs for the hexagonal and pentagonal arrays of Figures 20, 22, and 23 are shown in Figure 29. The bright spot at the core of the S = -2 disclination suggests that its core is a continuous core. There is a bright spot at the core of the S = -3/2 disclination. This disclination is expected to have a discontinuous core (Table 1) and thus this S = -3/2 disclination may not be a true S = -3/2 disclination, but disclinations of strength S = -1 and S = -1/2 next to each other.

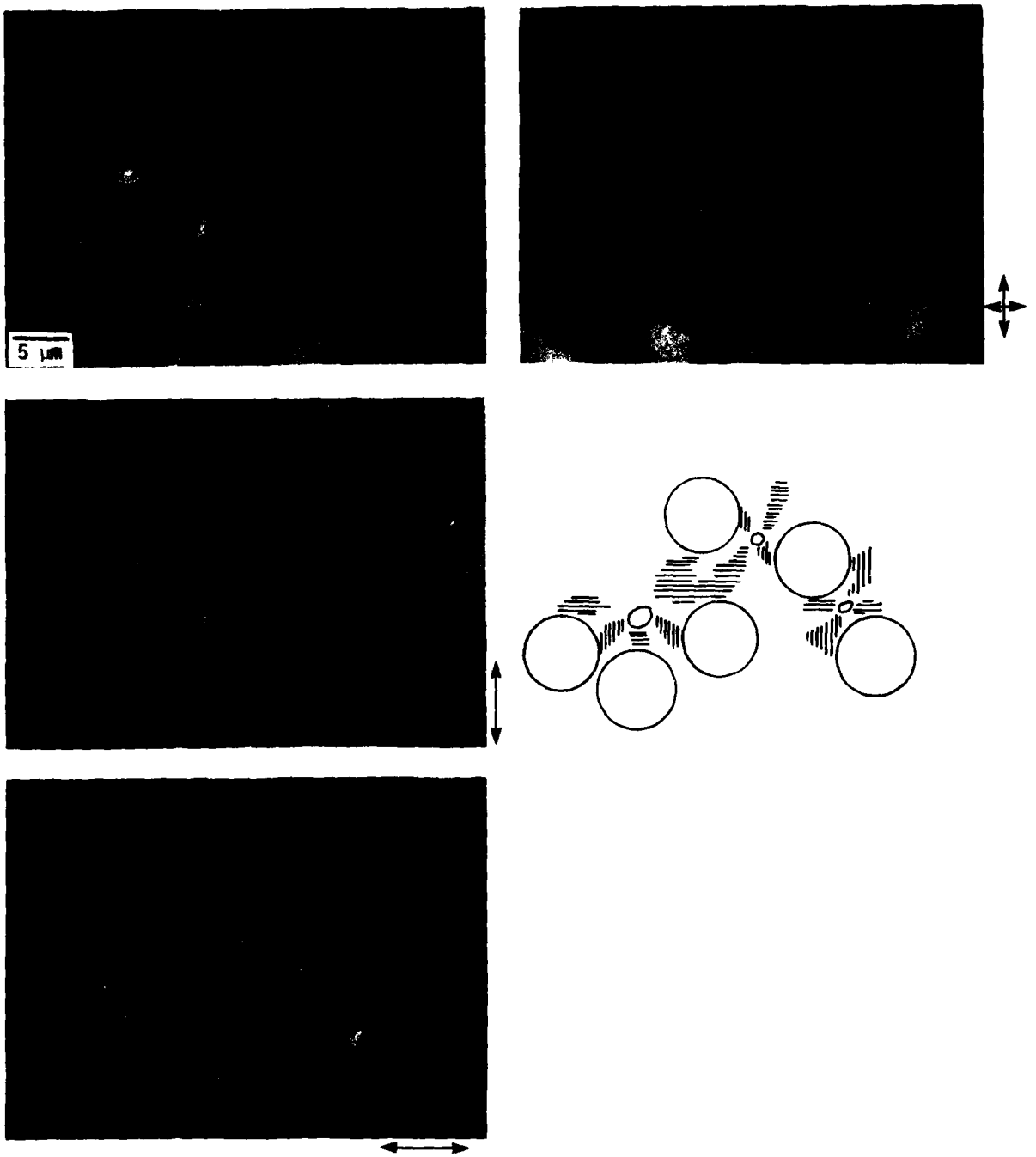

Figure 28. Micrographs with both bright-field and polarized light of disclinations in fiber bundle. The bright spots in the bright-field micrograph identify the continuous cores of the S = -1 disclinations.

A

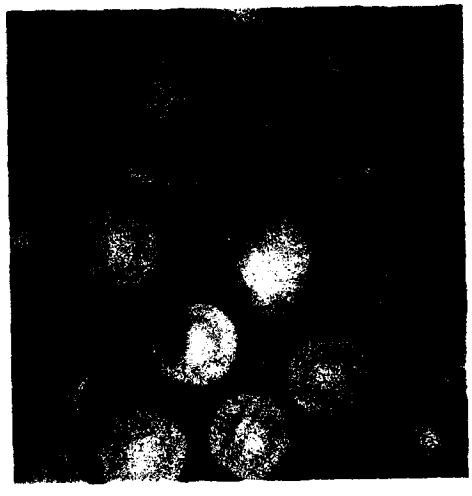

B

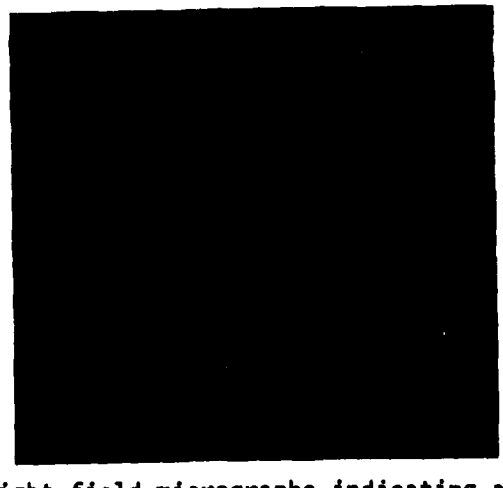

C

Figure 29. Bright field micrographs indicating a continuing core for the S = -2 disclinations (A, Figure 22 and B, Figure 23) and the S = -3/2 disclination (C, Figure 20).

Analysis of Core Structures

The configurations of the disclinations in the carbonaceous mesophase are defined by the curvature-elasticity theory developed by Frank [25]. The disclinations are singularities in a vectorfield of the normals to the disklike molecules at the condition of minimized free energy. Saupe [19] and Meyer [18] have extended this theory to determine the nature of the core structure of these disclinations. Applied to the wedge disclinations in a fiber bundle, this theory of the core structure is used here to predict the core structure of the disclinations in the carbonaceous mesophase and to further delineate the structure of the disclinations of higher strength.

The orientation of a disklike molecule is uniquely defined by its normal. For the disklike molecules in the mesophase that align parallel with long-range changes in the preferred orientation of the molecules, the normals define a vectorfield. Locally, the normals are aligned nearly parallel (Figure 30), but can exhibit curvatures of splay, twist and bend as shown in Figure 31. The vectorfield is a combination of these curvatures as space is mapped out by the normals to the disklike molecules. A three-dimensional vectorfield is quite complex. Each curvature has associated with it an elastic constant which is a measure of the ease or difficulty with which a curvature is formed as a result of an applied force. These elastic constants are termed K_1, splay; K_2, twist, and K_3, bend.

For a vectorfield with a certain state of imposed distortion (viscous flow, bubble percolation), the free-energy density of the liquid crystal is defined as

$$g = 1/2\ K_3(\text{div}\ \bar{n})^2 + 1/2\ K_2(\bar{n} \cdot \text{curl}\ \bar{n})^2 + 1/2\ K_1(\bar{n} \times \text{curl}\ \bar{n})^2 \quad . \quad (3)$$

As the elastic constants for the mesophase have not been measured, they are assumed equal here for simplicity. Then,

$$g = 1/2\ K[(\text{div}\ \bar{n})^2 + (\text{curl}\ \bar{n})^2] \qquad K = K_1 = K_2 = K_3 \tag{4}$$

The total free energy is

$$G = \int_V g\ dV \tag{5}$$

and at equilibrium, $\delta G = 0$.

For the vectorfield confined to a plane (x-y plane) such as the plane perpendicular to the fiber bundle, the normal vector is $\bar{n} = \cos\phi, \sin\phi$, where ϕ is the angle measured from the x-axis. The free-energy density is

$$g = 1/2\ K\left[\left(\frac{\partial\phi}{\partial x}\right)^2 + \left(\frac{\partial\phi}{\partial y}\right)^2\right] \tag{6}$$

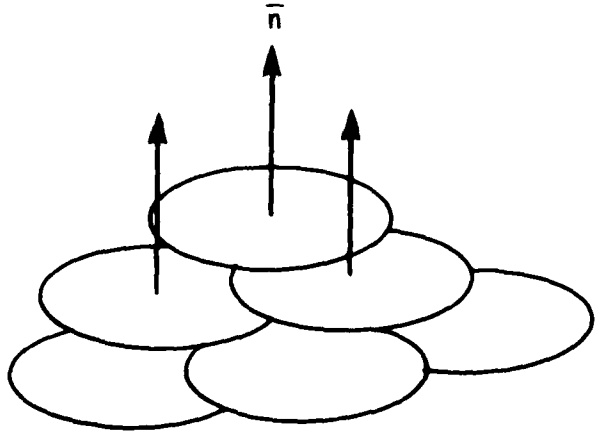

- Symmetry elements
  - -- any translation
  - -- any rotation about axis normal to molecules
  - -- a rotation of π about any axis parallel to molecules
- No point-to-point registry between adjacent molecules

Figure 30. Parallel stacking of disklike molecules.

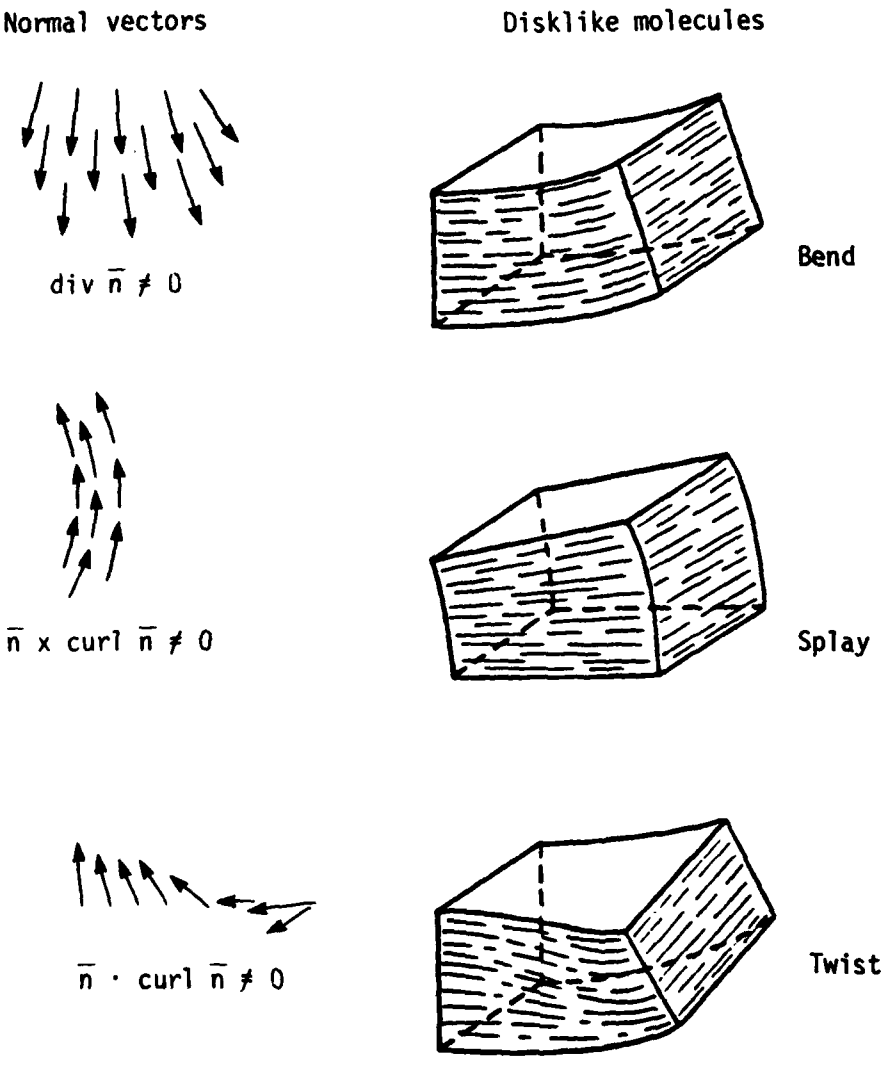

Figure 31. Curvatures of preferred orientation in the carbonaceous mesophase.

At equilibrium, minimization of the total free energy results in the relation,

$$\nabla^2 \phi = 0 \quad . \tag{7}$$

A set of solutions [25] to this equation that define the singularities in the vectorfield is

$$\phi = S\psi + \phi_0 \quad , \quad \psi = \tan y/x \quad , \; S = \pm 1/2, \pm 1, \; \ldots . \tag{8}$$

The configurations of the wedge disclinations of strength $S = \pm 1/2$ and $S = \pm 1$ by this equation are shown in Figure 2. The confinement of the normals to a plane forces the rotation vector and the disclination line to be parallel (to the z-axis). Thus this equation defines the wedge disclinations.

As previous research has shown [18, 19, 24], the wedge disclinations of integral strength ($S = \pm 1$) have continuous cores. Those with half-integral strength ($S = \pm 1/2$) have discontinuous cores. The analysis of the vectorfield in the core region is presented here and extended to include the disclinations of strength $S = \pm 3/2$ and $S = \pm 2$.

Consider a cylindrical region of liquid crystal about the disclination line. The normal to the molecules can tilt out of the x-y plane perpendicular to the disclination line. Thus, $\bar{n} = \sin\theta \cos\phi, \sin\theta \sin\phi, \cos\theta$ (Figure 32). With cylindrical coordinates, $x = r\cos\alpha$ and $y = r\sin\alpha$, the solutions to the Laplace equation (7), $\nabla^2\alpha = 0$, for the normal lying in the x-y plane are

$$\phi = S\alpha + \phi_0 \quad , \quad S = \pm 1/2, \; S = \pm 1 \quad , \ldots . \tag{9}$$

The equation for $\theta = \theta(r)$ is then a solution to

$$\frac{\partial^2\theta}{\partial r^2} + \frac{1}{r}\frac{\partial\theta}{\partial r} - \frac{S^2}{r^2}\cos\theta \sin\theta = 0 \tag{10}$$

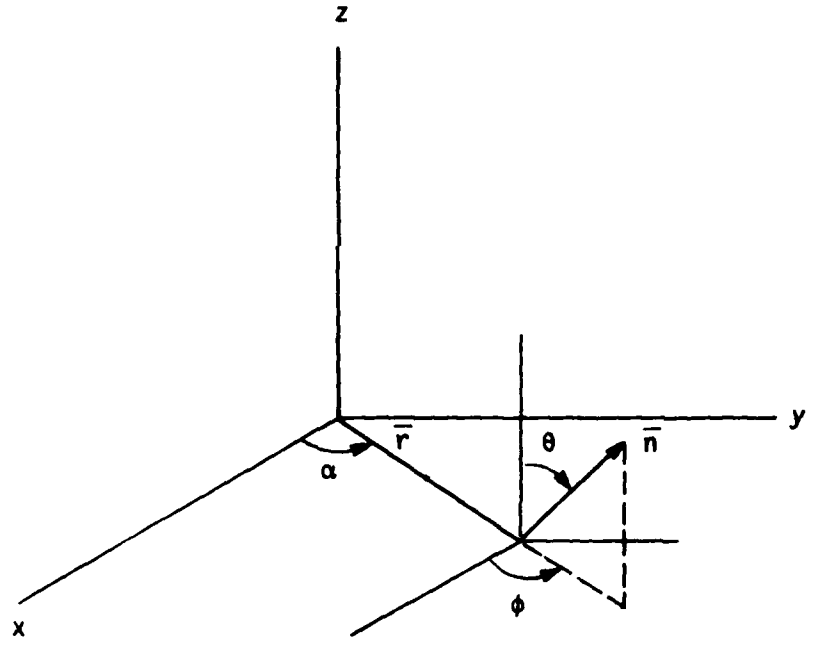

Figure 32. Coordinate system for vectorfield in core region of wedge disclination.

The boundary conditions are defined as follows. The normal lies in the x-y plane outside some core region of radius r_c; thus $\theta = \pi/2$ for $r = r_c$. At the center of the core, the normal is parallel to the z-axis, the disclination line: thus $\theta = 0$ for $r = 0$. In terms of the disklike molecules, the molecules at the center of the core are parallel to the x-y plane (perpendicular to the disclination line). Outside the core, the molecules are perpendicular to the x-y plane. The solution to this equation is

$$\tan \frac{\theta}{2} = \left(\frac{r}{r_c}\right)^{|S|} \tag{11}$$

With the use of a computer-graphics plotting program, the vectorfields for the wedge disclinations have been delineated by plotting equations (9) and (11) simultaneously. The wedge disclinations of strength $S = \pm 1$ and $S = \pm 2$ are shown in Figure 33. The change in molecular orientation through

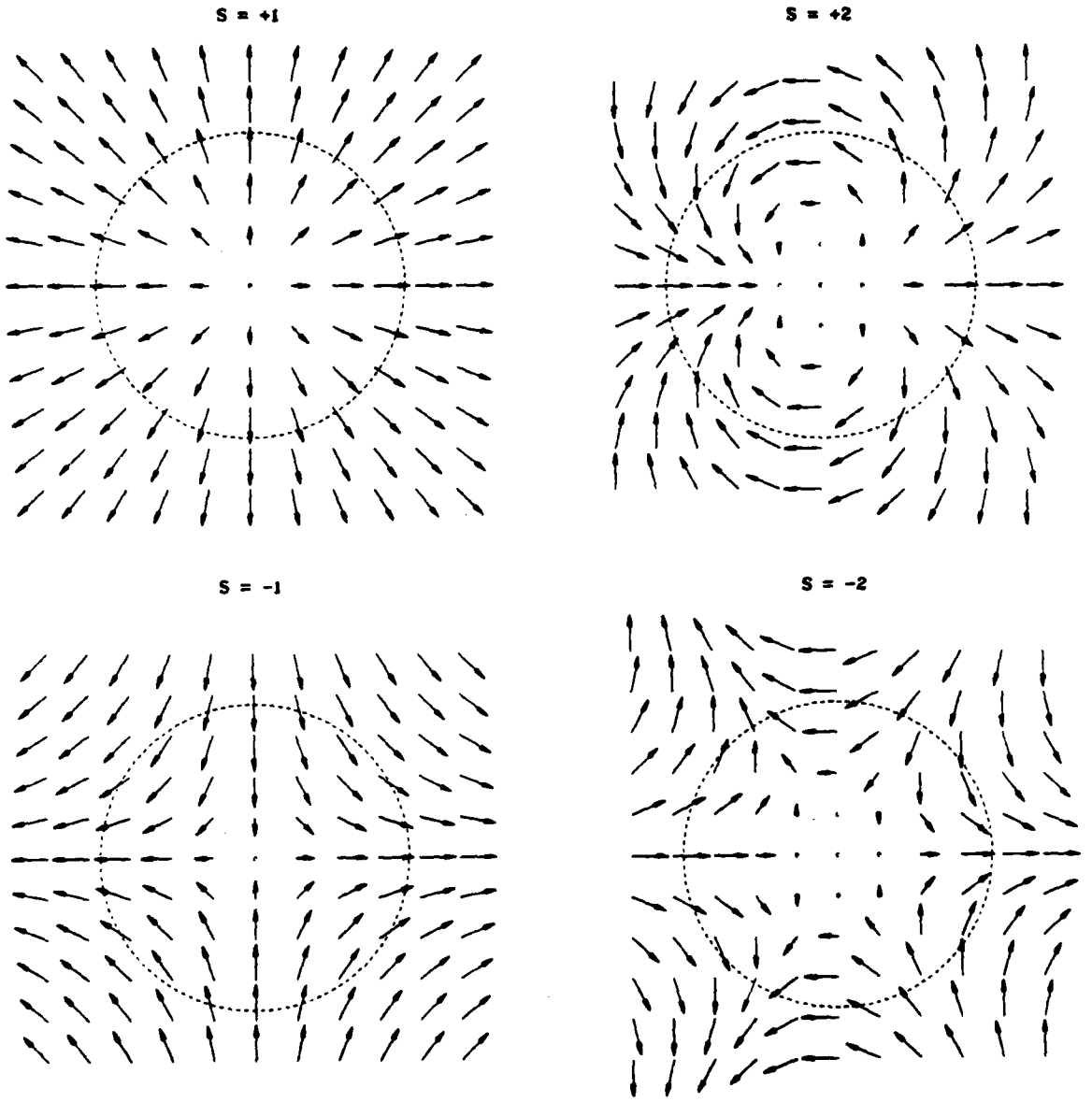

Figure 33. Vectorfield of normals to disklike molecules in the x-y plane perpendicular to the disclination line for disclinations of strength S = ±1 and S = ±2. The length of the unit vector is its projection on the plane and represents the angle it makes with the plane. The normals at the center of the core (dashed circle) are perpendicular to the plane.

the core is identified by the tilt of the vector out of the x-y plane (the change of length of its projection on the x-y plane). The continuous change in the orientation of the molecule normal is shown in Figure 34 for selected planes that are parallel to and contain the disclination line.

To further elucidate the structure of these core regions, the surfaces perpendicular to the vectorfield of normals were plotted with the use of the computer-graphics program. This surface is parallel the preferred direction of the disklike molecules. The core structures of the wedge disclinations of strength $S = \pm 1$ and $S = \pm 2$ are shown in Figure 35. The core structure of the $S = \pm 1$ disclination is cup-shaped (cf. Figure 26) and the core structure of the $S = -1$ disclination is saddle-shaped (cf. Figure 27). Most interesting are the core structures of the disclinations of strength $S = \pm 2$. Although the $S = +2$ disclination has not been observed in the mesophase, its core structure should have this chair-shaped surface. The core structure of the $S = -2$ disclination, which has been observed in the hexagonal array of filaments in a fiber bundle, has a complex saddle shape, a three-legged saddle.

This analysis of the core structure of the $S = -1$ and $S = -2$ wedge disclinations and the definition of a continuous core structure for each, conducted to support of the experimental evidence, strongly indicates that the disclination of strength $S = -2$ does exist and has a continuous core structure. Its existence is made possible by the unique alignment of filaments (hexagonal array) in a fiber bundle. Evidence for the $S = +2$ disclination will require another imposed geometry for the carbonaceous mesophase.

The surfaces of the core structure of the half-integer disclinations have been defined in the same manner by plotting equations (9) and (11) with the boundary condition that the molecules are perpendicular to the

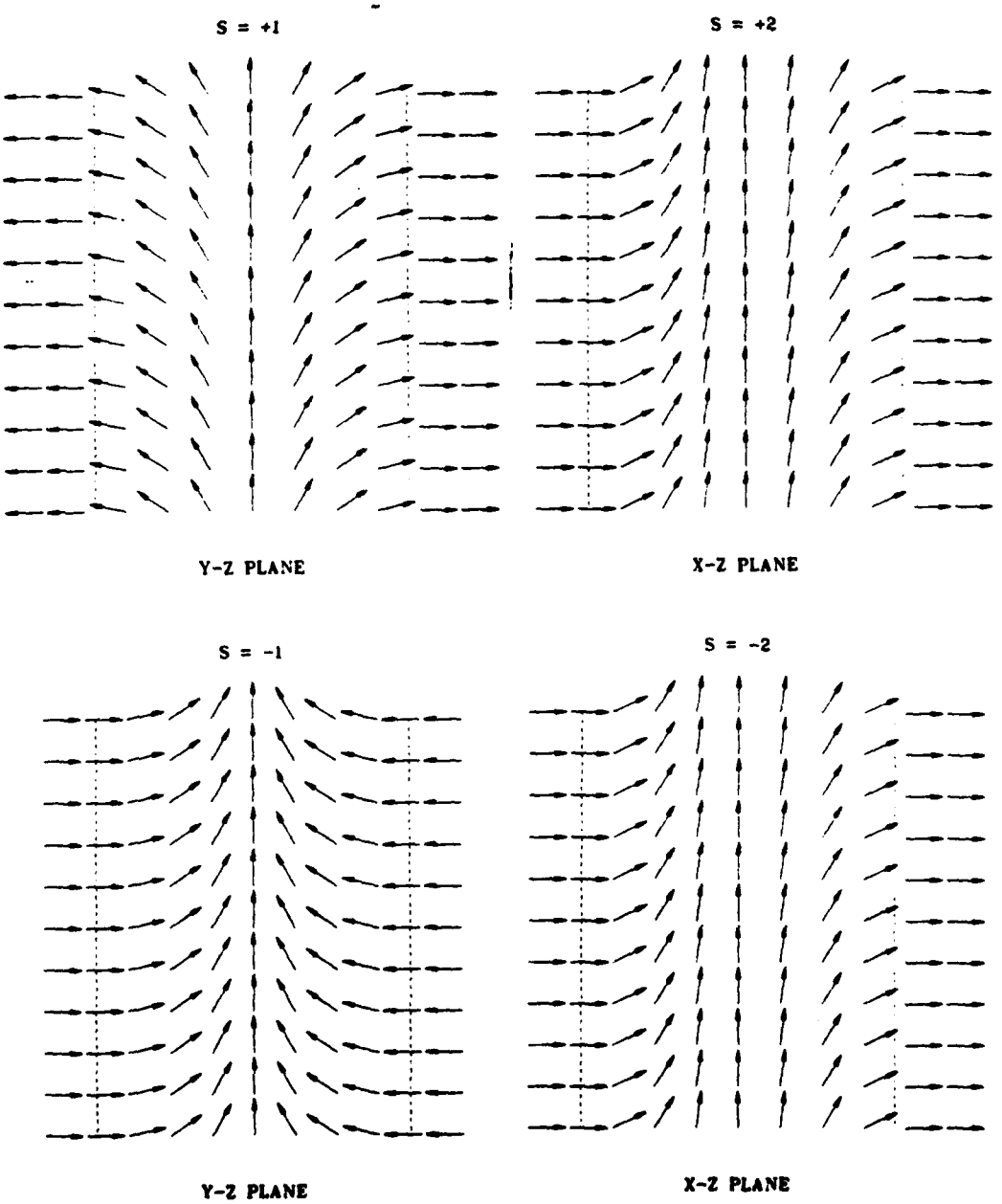

Figure 34. Configuration of core structure of wedge disclinations of strength S = ±1 and S = ±2 on planes parallel to the disclination line.

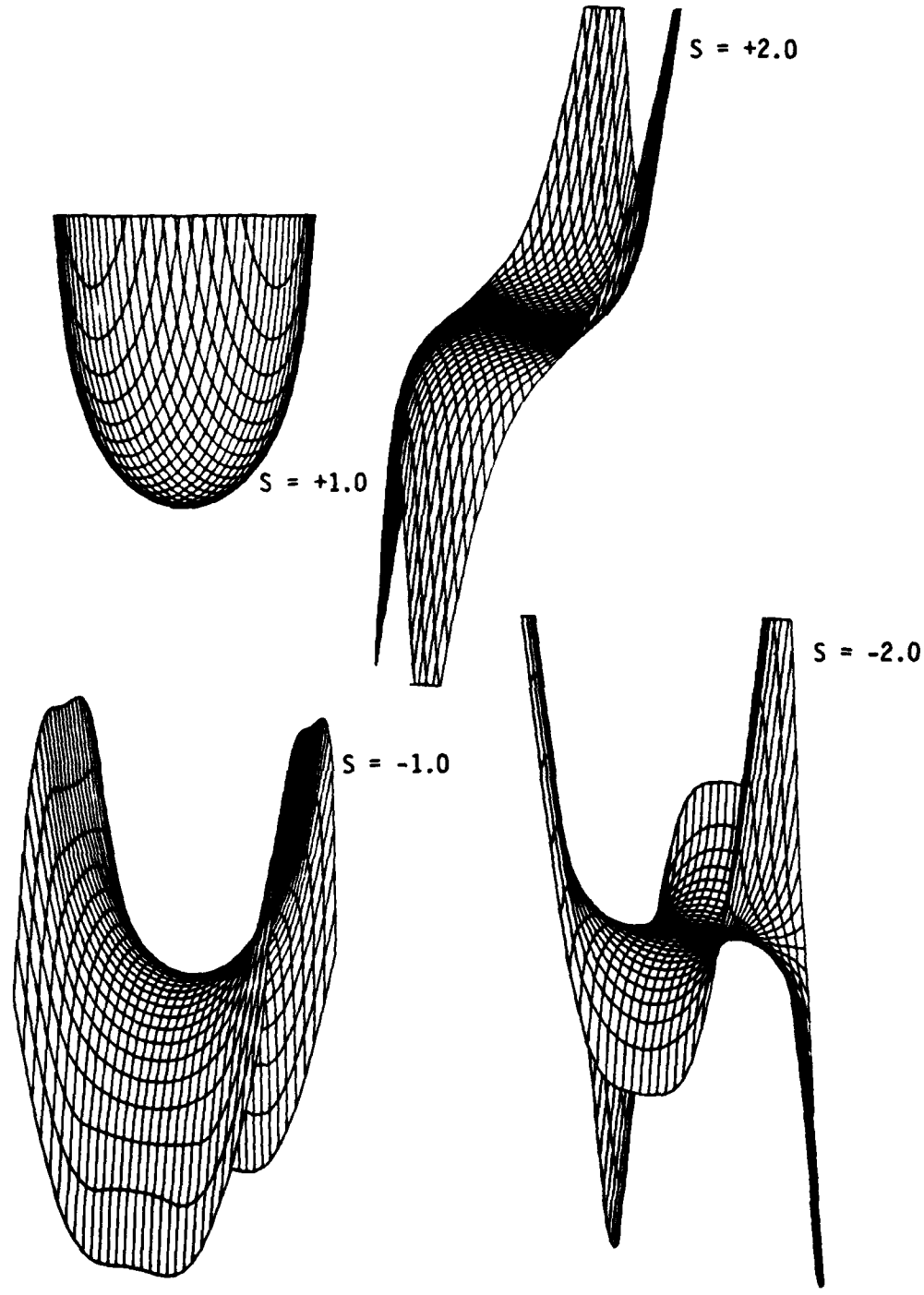

Figure 35. The surface representing the orientation of the molecules in the core region of the wedge disclinations of strength S = ±1 and S = ±2. The wedge disclination is vertical and in the center of each surface.

disclination line at the center of the core. These surfaces are shown in Figure 36 for the wedge disclinations of strength $S = \pm 1/2$ and $S = \pm 3/2$. The discontinuity or tear in these surfaces implies that the equations and imposed boundary conditions do not apply for these disclinations. Thus, the cores of these half-integer disclinations are not continuous, but must be discontinuous. The vectorfield for these disclinations is shown in Figure 37, without the imposed boundary conditions for a continuous core. Normals to all the molecules lie in the plane perpendicular to the disclination line and thus these disclinations have discontinuous cores.

The existence of a wedge disclination of strength $S = -3/2$ in a pentagonal array in a fiber bundle is possible. In a bright-field micrograph, the core of the $S = -3/2$ disclination will not show as a bright spot, as is the case for the $S = -1/2$ disclination. The evidence here for the $S = -3/2$ disclination (Figures 20 and 29) suggests that this is not an $S = -3/2$ disclination. The search for this disclination will continue.

The change in molecular orientation throughout the continuous cores of the integral-strength disclinations reduces the energy of these disclinations [18, 19]. For the disclinations in a fiber bundle, the ratio of the distance between disclinations (R) and a core radius (r_o) is about 30. Thus, the energy of the wedge disclinations as defined by equation (1) is

$$E = 3.4\pi KS^2 + E_{core}$$

For the energy of a discontinuous core of about K [19], this disclination energy is then

$$E = 4.4\pi KS^2 \quad .$$

Meyer [19] has shown that the energy of the $S = 1$ disclinations with continuous cores is $E = 3\pi K$, which is less than $4.4\pi K$ if the core is assumed to be discontinuous.

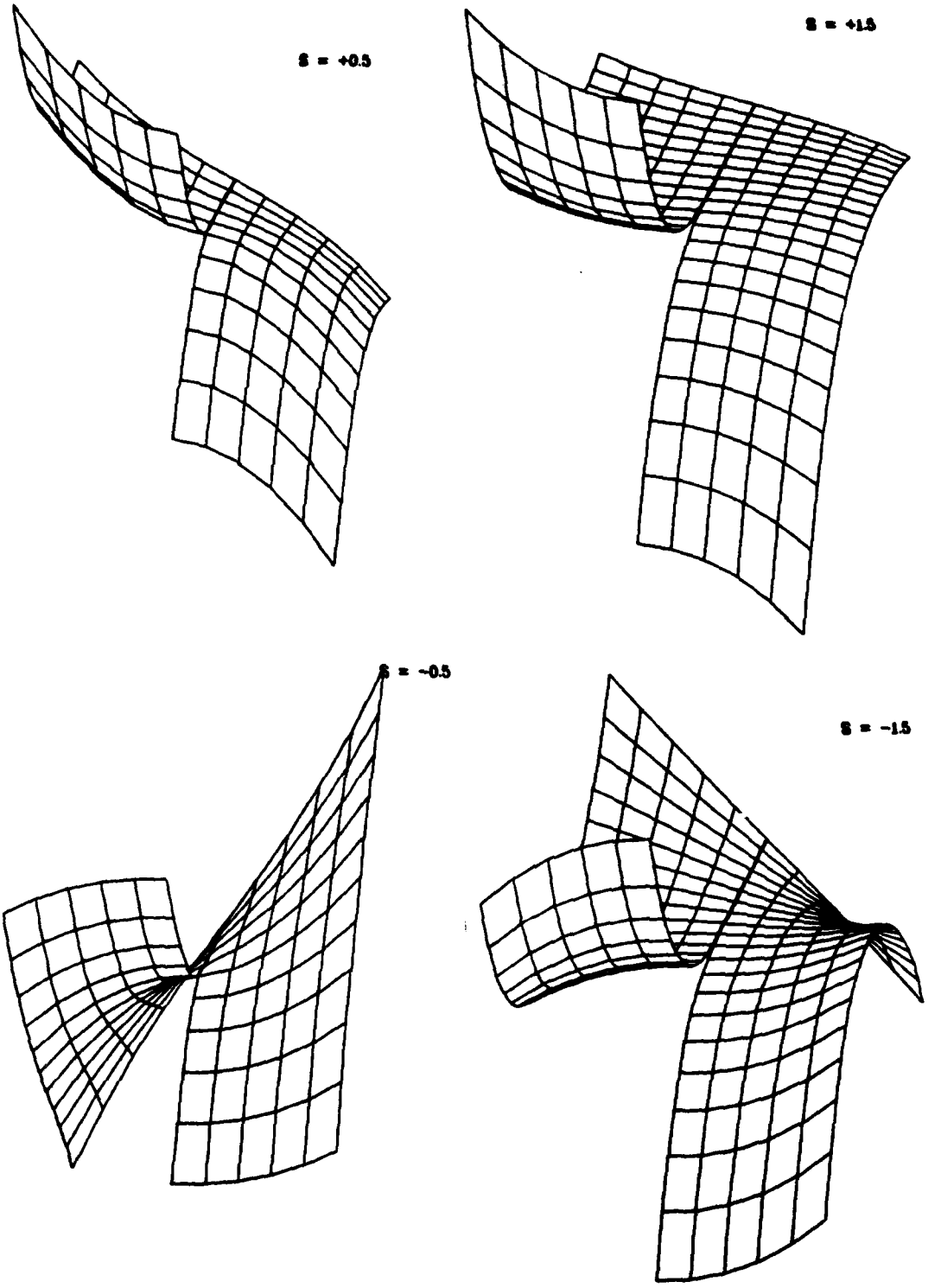

Figure 36. Surfaces in the core region of the S = ±1/2 and S = ±3/2 wedge disclinations. The discontinuity, where the normal changes sign abruptly, suggests that these disclinations do not have continuous cores.

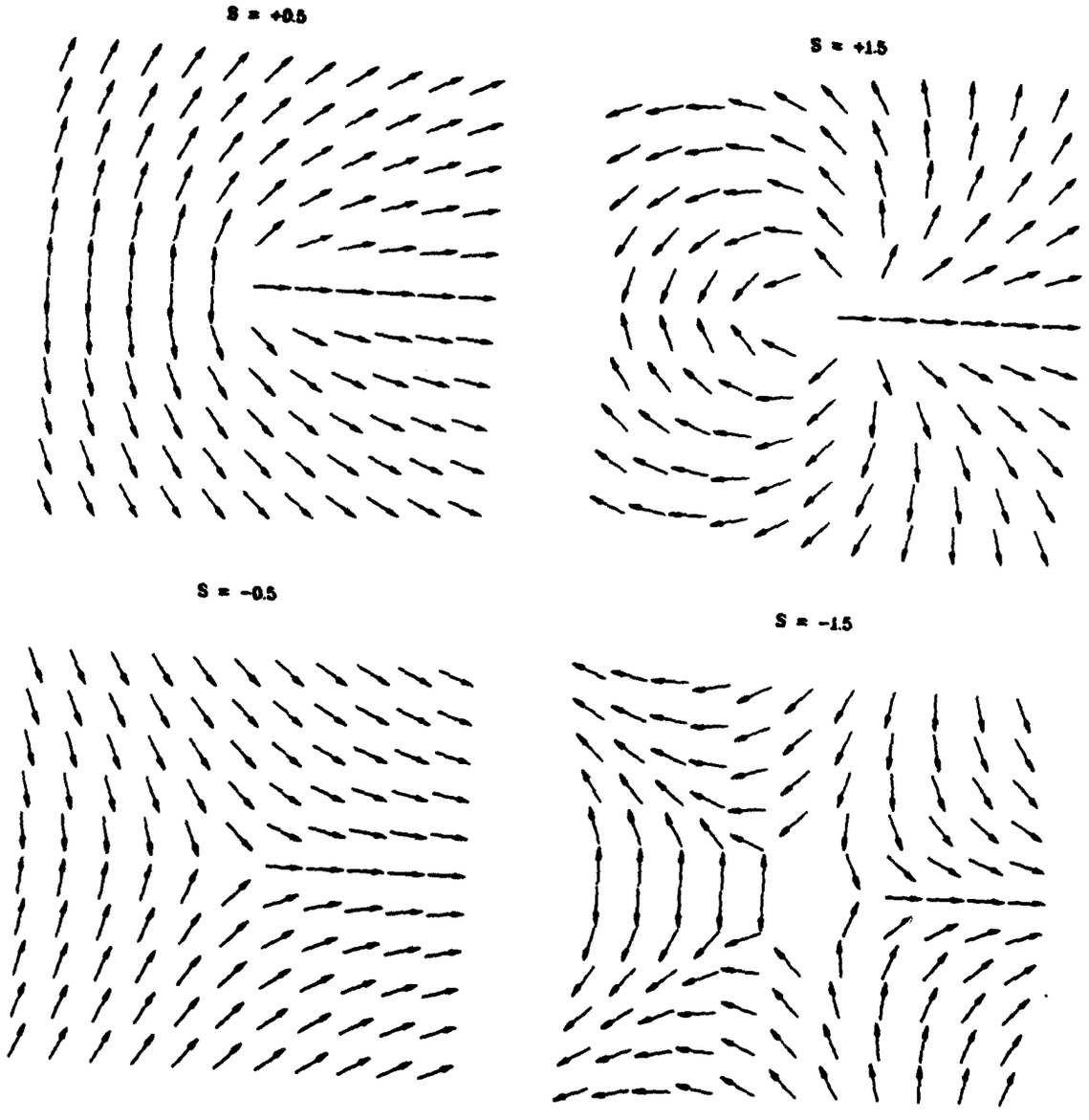

Figure 37. Vectorfield of normals to disklike molecules in the plane perpendicular to the disclination line for disclinations of strength S = ±1/2 and S = ±3/2. These disclinations have discontinuous cores.

PUBLICATIONS

The following technical publications have been prepared with support in part by this research program:

1. J. E. Zimmer, and J. L. White, Advances in Crystals 5, 157 (1982). A review article entitled "Disclination Structures in the Carbonaceous Mesophase."
2. J. E. Zimmer, and J. L. White, Carbon, in preparation. A letter to the editor entitled "Mesophase Alignment Within Carbon-Fiber Bundles."
3. J. E. Zimmer, "Disclinations and Fracture," presentation at International Symposium on Carbon, 1-4 November 1982, Toyohashi, Japan.

REFERENCES

1. J. D. Brooks and G. H. Taylor, Chem. and Phys. of Carbon 4, 243 (1965).
2. J. L. White, Progr. in Solid State Chem. 9, 59 (1975).
3. J. L. White and J. E. Zimmer, Surface and Defect Properties of Solids 5, 16 (1976).
4. I. Mochida, K. Maeda and K. Takeshita, Carbon 16, 459 (1978).
5. F. R. N. Nabarro, Theory of Crystal Dislocations, Clarendon Press, Oxford (1967).
6. V. Volterra, Ann. Sci. Ecole Norm. Super., Paris, 24, 401 (1907).
7. J. L. White, G. L. Guthrie, and J. O. Gardner, Carbon 5, 517 (1967).
8. J. E. Zimmer and J. L. White, Mol. Cryst. Liq. Cryst. 38, 177 (1977).
9. J. L. White and J. E. Zimmer, Carbon 16, 469 (1978).
10. J. E. Zimmer, Ph.D. Thesis, Purdue University, 1978.
11. A. Saupe, Mol. Cryst. Liq. Cryst. 21, 211 (1973).
12. G. S. Ranganath, Mol. Cryst. Liq. Cryst. 34, 71 (1976).
13. S. F. Pugh, Brit. J. Appl. Phys. 18, 129 (1967).
14. J. E. Brocklehurst, Chem. and Phys. Carbon 13, 145 (1977).
15. G. D. Swanson, J. Amer. Ceram. Soc. 55, 48 (1972).
16. J. D. Brooks and G. H. Taylor, Carbon 3, 185 (1965).
17. J. Dubois, C. Agace, and J. L. White, Metallography 3, 337 (1970).
18. R. B. Meyer, Phil. Mag. 27, 405 (1973).
19. A. Saupe, Mol. Cryst. Liq. Cryst. 21, 211 (1973).

20. C. E. Williams, P. E. Cladis and M. Kleman, Mol. Cryst. Liq. Cryst. 21, 355 (1973).

21. P. E. Cladis and M. Kleman, J. de Phys. 33, 591 (1972).

22. C. E. Williams, P. Pieranski and P. E. Cladis, Phys. Rev. Let. 29, 90 (1972).

23. R. B. Meyer, Mol. Cryst. Liq. Cryst. 16, 355 (1972).

24. J. E. Zimmer and J. L. White, Extended Abstracts, 14th Conf. on Carbon, 429 (1979).

25. F. C. Frank, Discussion Faraday Society 25, 19 (1958).

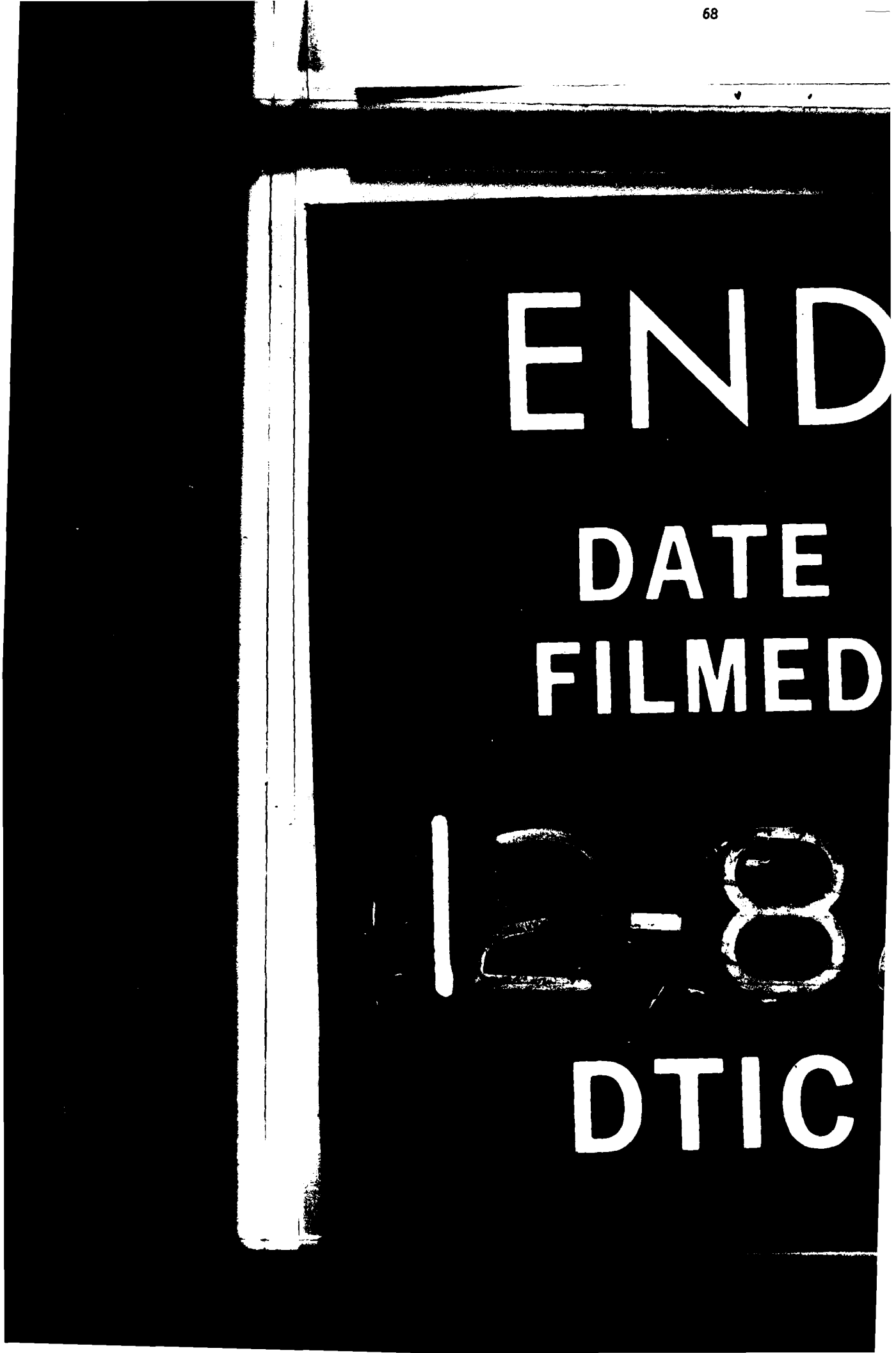
END
DATE
FILMED
12-8
DTIC